The impact of demography in a model of malaria with Transmission Blocking Drugs

R. Ouifki[1], J. Banasiak[2,3] and S. Y. Tchoumi[2,4]

1. Department of Mathematics and Applied Mathematics, North West University, Mahikeng, South Africa
2. Department of Mathematics and Applied Mathematics, University of Pretoria, Pretoria, South Africa
3. Institute of Mathematics, Łódź University of Technology, Łódź, Poland
4. Department of Mathematics and Computer Sciences ENSAI, University of Ngaoundere, Ngaoundere, Cameroon.

Abstract

In this paper, we develop and analyze a mathematical model for spreading malaria, including treatment with Transmission Blocking Drugs (TBDs). The paper's main aim is to demonstrate the impact the chosen model for demographic growth has on the disease's transmission and the effect of its treatment with TBDs. We calculate the model's control reproduction number and equilibria, and perform a global stability analysis of the disease-free equilibrium point. The mathematical analysis reveals that, depending on the model's demography, the model can exhibit forward, backward and even some unconventional types of bifurcation, where disease elimination can occur for both small and large values of the reproduction number. We also conduct a numerical analysis to explore the short-time behavior of the model. A key finding is that for one type of demographic growth, the population experienced a significantly higher disease burden than the others, and when exposed to high levels of treatment with TBDs, only this population succeeded in effectively eliminating the disease within a reasonable timeframe.

Keywords: Transmission blocking drugs, mathematical modeling, demography, malaria, simulation.

1   Introduction

Malaria is a vector-borne infectious disease caused by infection with single-celled protozoan parasites of the genus *Plasmodium* — single-celled organisms that cannot survive outside their host(s). Malaria pathology is caused by repeated reproduction of the parasites in the human red blood cells. The sporozoites, the transmissible stage of *Plasmodium* parasite residing within the mosquito mid-gut, are transmitted to humans through bites of infected female *Anopheles* mosquitoes (vectors) when they feed on human blood [27, 43]. *Anopheles* mosquitoes become infected when they feed and ingest human blood that contains mature gametocytes, the transmissible stage of the *Plasmodium* parasite within human.

Despite malaria being preventable and treatable, it remains one of the most prevalent and deadliest human infections in developing countries, especially in Sub-Saharan Africa, where young children and pregnant women are most affected [33, 40]. According to the WHO malaria report (2020) [41], there were an estimated 241 million cases of malaria worldwide in 2020, resulting in around 627 thousand deaths. The WHO African region carries a disproportionately high share of the global malaria burden with as much as 95% of malaria cases and 96% of malaria deaths, where 80% we are children, recorded in Africa in 2020, [41].

Increased investment and research on malaria control interventions have resulted in impressive reductions in global malaria cases and mortality, see Figure 1. Sub-figure 1(b) shows that the number of malaria-caused deaths has continued to decrease globally and in Africa for the years $2010 - 2017$. Particularly, it can be estimated from the data that the number of malaria-caused deaths in Africa has fallen by approximately 27.4% in 2015 compared to 2017. However, in sub-figure 1(a), the number of malaria cases decreased in the years $2010 - 2015$, but it started to increase in the years $2015 - 2017$, even though the malaria cases in 2010 was still higher than in any year from 2010 to 2017. Specifically, the number of malaria cases in Africa has fallen approximately by 6.1% in 2015 compared to 2010. However, there was an approximately 2.4% increase in the number of malaria cases in Africa in 2017 compared to the year 2015, see Figure 1.
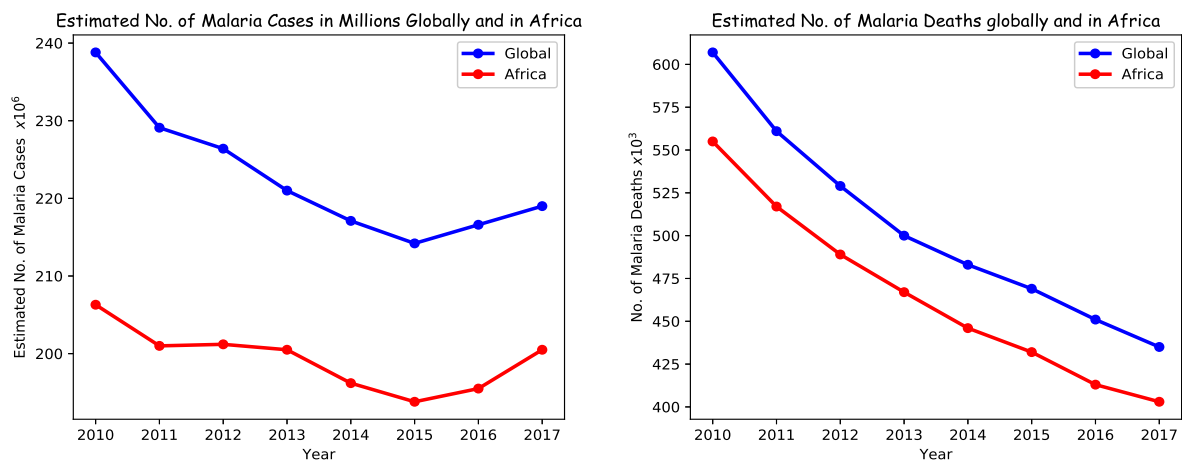
(a) Estimated number of malaria cases by WHO in Africa and globally

(b) Estimated number of malaria deaths by WHO in Africa and globally

Figure 1: Visualization of data obtained from the World Health Organization (WHO)-Global Health Observatory (GHO) [42] for the estimated number of cases and deaths for $2010 - 2017$. We used Python programming language to plot these figures using the data obtained from WHO-GHO, [42].

Despite the reduction of the number of disease-caused deaths, malaria remains a major global health problem, and there is empirical and theoretical evidence that the current suite of interventions alone will not be sufficient to eliminate it in most endemic areas, particularly in Sub-Saharan Africa, [24]. Novel intervention strategies need to be considered. Recently, several researchers and scientists have shifted their research to new in-host transmission-blocking interventions (TBIs) such as transmission-blocking drugs (TBDs) and vaccines (TBVs), [7, 15]. It is expected that new medicines that block transmission and target dormant reservoirs of the malaria parasite, such as the hypnozoite of *P. vivax*, will have an important role in the eradication of malaria.

As mentioned in [39], TBDs can be drugs targeting the malaria parasite within the human host, the parasite in the vector, or the vector itself. Such drugs are designed to be administered to humans so that during the blood meal, the mosquito will take them together with the blood, [44]. Transmission-blocking properties of common drugs have been known for some time. However, to eradicate malaria, it was necessary to develop drugs specifically designed to completely block *Plasmodium* parasites transmission, [3], and there are many promising clinical advances in the development of such novel TBDs, see [3, 7, 15, 39]. Also the use of TBDs to target the reservoir of malaria infection plays an important role in reducing or possibly stopping the transmission of malaria between humans and mosquito vectors.

Many epidemiologists and other scientists have invested their efforts in learning malaria's dynamics

and controlling its transmission. An impressive variety of biological literature and epidemiological models exist to study the immuno-pathogenesis and dynamics of malaria transmission. The use of mathematical models increases the impact of the theory on the practices of disease management and control, see, e.g., [2, 5, 10, 11, 13, 14, 17, 25, 30, 31, 35, 37, 1, 6, 9, 18, 45].

Moreover, given the pivotal role that demographic factors play in shaping the transmission dynamics and control of infectious diseases, a multitude of mathematical models for infectious diseases have incorporated various demographic structures, revealing their significant impact on the dynamics and control of diseases (refer to [19, 20, 26, 21, 36, 12, 28] for further insights). For an extensive and systematic review of models that incorporate dynamic population structures into infectious disease transmission models, we refer to the work of [29]. Therefore, the incorporation and thorough examination of various types of demographic growths within malaria modeling is essential for enhancing the understanding of disease transmission and the design and implementation of effective control measures using TBDs.

Hence, in this paper, we propose a novel minimalistic mathematical model for malaria with TBDs, which nevertheless captures the essential aspects of TBDs, and analyze the impact of the chosen demographic model on the disease's transmission and its control with the drugs. We provide a mathematical analysis of the model and present comprehensive numerical simulations to reveal the impact of the demography on its short- and long-term behavior.

The paper is organized as follows. In section 2, we formulate the model, and in section 3, we present its mathematical analysis. In particular, in subsection 3.2, we determine the disease-free equilibrium point and study the dependence of the number of replications on the treatment coverage rate and the efficacy of TBDs; in subsection 3.4, we carry out a rigorous study of the existence and number of endemic equilibria for the different types of population growth and the possibilities of occurrence of bifurcations and in the subsection 3.5, we prove the global asymptotic stability of the disease-free equilibrium. In section 4, we present numerical results that illustrate the effect of treatment with TBDs and the impact of population growth in malaria dynamics. The paper ends with conclusions in section 5.

2 The model

We propose a simplified model of malaria transmission using treatment with TBDs, which, nevertheless, captures the essential features of the treatment by introducing the protected class. Thus, the human population is subdivided into four compartments: susceptible (S_h), infectious (I_h), recovered (R_h) and protected (P_h). On contact with an infectious mosquito, a susceptible human can become infectious at the rate $\frac{a\beta_{vh}I_v}{N_h}$. Once infectious, the individual may recover naturally at the rate σ, joining the recovered class, or may recover after treatment with a TBD at the rate ω_h, thus becoming protected, that is noninfective and immune. Recovered individuals may lose their immunity at the rate of γ_h, and protected individuals may lose their protection at the rate of ϑ_h. All individuals may die at the rate $d_h(N_h)$, and infectious individuals can also die of the disease at the rate δ_h. We consider four demographic models for the human population

a) Malthusian growth,
$$b_h(N_h) = \pi_h N_h, \quad d_h(N_h) = \mu_{1h}.$$

b) Simplified logistic, or affine, growth,
$$b_h(N_h) = \lambda_h, \quad d_h(N_h) = \mu_{1h}.$$

c) Logistic growth — density dependent birth rate,

$$b_h(N_h) = r N_h \left(1 - \frac{N_h}{K}\right), \quad d_h(N_h) = \mu_{1h}.$$

d) Logistic growth — density dependent death rate,

$$b_h(N_h) = \pi_h N_h, \quad d_h(N_h) = \mu_{1h} + \mu_{2h} N_h.$$

In the mosquito population, a susceptible mosquito in contact with an infectious individual or a recovered individual can become infectious at the rate $\dfrac{a\beta_{hv}(I_h + \xi_r R_h)}{N_h}$, and all mosquitoes die at the rate $d_v(N_v)$.

Recruitment to humans and mosquitoes occurs only in the susceptible class and is described by the functions $b_h(N_h)$ and $b_v(N_v)$, respectively.

The descriptions of the compartments in model (1) with TBDs is given in Table 1.

Variables	Description	Quasi-dimension
S_h	susceptible humans	H
I_h	infectious humans	H
R_h	recovered humans	H
P_h	protected, i.e., successfully treated and noninfective humans	H
S_v	susceptible mosquitoes	V
I_v	infectious mosquitoes	V

Table 1: State variables, their description and corresponding quasi-dimension.

The flow of the model is shown on Fig. 2, while the parameters are described in Table 2.
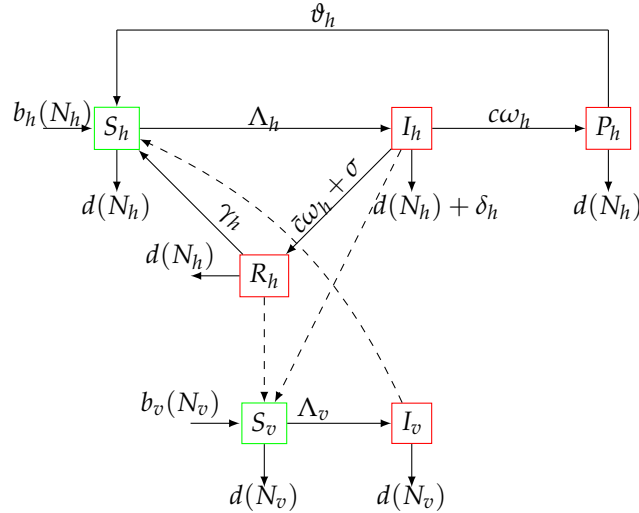

Figure 2: Flow diagram showing the malaria transmission dynamics between human and mosquito populations with a transmission-blocking drug treatment, Here $\bar{c} = 1 - c$, $b_h(N_h)$ and $b_v(N_v)$ represent the net rates of births, whereas $d_h(N_h)$ and $d_v(N_v)$ represent the net rates of deaths for humans and vectors, respectively. Description of the parameters of the model is given in Table 2.

Table 2: Parameters, their description and corresponding quasi-dimension. We use the notations H for dimension of number humans, V for number of mosquito-vectors.

Parameters	Description	Quasi-dimension
λ_h	total constant recruitment rate of susceptible humans	$H \times day^{-1}$
π_h	per capita birth rate of humans	day^{-1}
π_v	per capita birth rate of mosquitoes	day^{-1}
β_{vh}	the probability of transmission from infectious vector (mosquito) to susceptible humans during bite	dimensionless
β_{hv}	the probability of transmission from infectious humans to susceptible vectors during bite	dimensionless
a	the average biting rate of mosquitoes on humans	$H \times (V \times day)^{-1}$
Λ_h	force of infection from infectious vectors to susceptible humans	day^{-1}
Λ_v	force of infection from infectious humans to susceptible vectors	day^{-1}
ω_h	constant rate of treatment of infectious human with TBD	day^{-1}
c	probability that TBDs confer 100% reduction in transmission	dimensionless
γ_h	waning rate of immunity	day^{-1}
σ	natural recovery rate of infected humans by immune response	day^{-1}
ζ_r	reduction of the infectivity of recovered humans to vectors	dimensionless
μ_{1h}	density-independent death rate of humans	day^{-1}
μ_{1v}	density-independent death rate of mosquitoes	day^{-1}
μ_{2h}	additional density-dependent part of the death rate for humans	$H^{-1} \times day^{-1}$
μ_{2v}	additional density-dependent part of the death rate for mosquitoes	$V^{-1} \times day^{-1}$
δ_h	disease induced death rate	day^{-1}
ϑ_h	rate at which individuals in class P_h lose their protection against infection	day^{-1}

Therefore, we shall study the following non-linear system of ODEs.

$$
\begin{cases}
S_h' = b_h(N_h) + \gamma_h R_h + \vartheta_h P_h - \left(a\beta_{vh}\frac{I_v}{N_h} + d_h(N_h) \right) S_h, \\[2mm]
I_h' = a\beta_{vh}\frac{I_v}{N_h} S_h - (\omega_h + \sigma + d_h(N_h) + \delta_h) I_h, \\[2mm]
R_h' = ((1-c)\omega_h + \sigma) I_h - (\gamma_h + d_h(N_h)) R_h, \\[2mm]
P_h' = c\omega_h I_h - (\vartheta_h + d_h(N_h)) P_h, \\[2mm]
S_v' = b_v(N_v) - \left(a\beta_{hv}\frac{(I_h + \zeta_r R_h)}{N_h} + d_v(N_v) \right) S_v, \\[2mm]
I_v' = a\beta_{hv}\frac{(I_h + \zeta_r R_h)}{N_h} S_v - d_v(N_v) I_v
\end{cases}
\tag{1}
$$

with initial conditions

$$
\begin{cases}
S_h(0) > 0, \quad I_h(0) \geq 0, \quad R_h(0) \geq 0, \quad P_h(0) \geq 0, \\
S_v(0) > 0, \quad I_v(0) \geq 0.
\end{cases}
\tag{2}
$$

3 Analysis of the model

In the next subsection, we present various results on the mathematical analysis of the model (1).

3.1 Basic properties of the model

In this subsection, we find the invariant region of the model (1) and, in particular, non-negativity of its solutions. To simplify the expressions, we let $g_i(N_h) = \omega_h + \sigma + \delta_h + d_h(N_h)$, $g_r(N_h) = \gamma_h + d_h(N_h)$ and

$g_p(N_h) = \vartheta_h + d_h(N_h)$, $A_h = a\beta_{vh}$, $A_v = a\beta_{hv}$ and $f_r = (1-c)\omega_h + \sigma$.

Proposition 1 *The non-negative cone $\mathbb{R}^6_+$ is positively invariant for the system* (1) *with initial conditions* (2).

Proof. The system model (1) can be written in a matrix form as

$$\mathbf{x}' = \mathbf{A}(\mathbf{x})\mathbf{x} + \mathbf{b}(\mathbf{x}),$$

where $\mathbf{x} = (S_h, P_h, S_v, I_h, I_v, R_h)^T$, $\mathbf{b}(\mathbf{x}) = (b_h(N_h), b_v(N_v), 0, 0, 0, 0)^T$ and

$$\mathbf{A}(\mathbf{x}) = \begin{pmatrix} -\dfrac{A_h I_v}{N_h} - d_h(N_h) & \vartheta_h & 0 & \gamma_h & 0 & 0 \\ 0 & -g_p(N_h) & 0 & c\omega_h & 0 & 0 \\ 0 & 0 & -\dfrac{A_v(I_h + \xi_r R_h)}{N_v} - d_h(N_v) & 0 & 0 & 0 \\ 0 & 0 & 0 & -g_i(N_h) & \dfrac{A_h S_h}{N_h} & 0 \\ 0 & 0 & 0 & \dfrac{A_v S_v}{N_h} & -d_v(N_v) & \dfrac{\xi_r A_v S_v}{N_h} \\ 0 & 0 & 0 & f_r & 0 & -g_r(N_h) \end{pmatrix}.$$

The matrix $\mathbf{A}$ is Metzler matrix and it is well know that the systems determined by Metzler matrices preserve invariance of the non-negative cone. ∎

The time derivatives of the total human population $N_h(t)$ and mosquitoes $N_v(t)$ can be obtained by adding the first fourth and, respectively, the last two, equations, of system (1):

$$\begin{cases} N_h' = b_h(N_h) - d_h(N_h)N_h - \delta_h I_h, \\[2mm] N_v' = b_v(N_v) - d_v(N_v)N_v. \end{cases} \tag{3}$$

Therefore often we will find it advantageous to work with the following version of (1)

$$\begin{cases} N_h' = b_h(N_h) - d_h(N_h)N_h - \delta_h I_h, \\[1mm] I_h' = a\beta_{vh}\frac{I_v}{N_h}(N_h - I_h - R_h - P_h) - (\omega_h + \sigma + d_h(N_h) + \delta_h)I_h, \\[1mm] R_h' = ((1-c)\omega_h + \sigma)I_h - (\gamma_h + d_h(N_h))R_h, \\[1mm] P_h' = c\omega_h I_h - (\vartheta_h + d_h(N_h))P_h, \\[1mm] N_v' = b_v(N_v) - d_v(N_v)N_v, \\[1mm] I_v' = a\beta_{hv}\frac{(I_h + \xi_r R_h)}{N_h}(N_v - I_v) - d_v(N_v)I_v. \end{cases} \tag{4}$$

Proposition 2 *Let N_h^0 and N_v^0 be the positive constant equilibrium of the system* (3) *when all the infectious components are zero. The set $\Omega = \Omega_h \times \Omega_v \subseteq \mathbb{R}^4_+ \times \mathbb{R}^2_+$, where*

$$\Omega_h = \left\{(N_h, I_h, R_h, P_h) \in \mathbb{R}^4_+ : 0 < S_h + I_h + R_h + P_h \leq N_h^0\right\},$$
$$\Omega_v = \left\{(S_v, I_v) \in \mathbb{R}^2_+ : 0 < S_v + I_v \leq N_v^0\right\}.$$

is positively invariant and attracts all solutions to system (1) *emanating from $\mathbb{R}^{6*}_+$.*

3.2 Disease free equilibrium and basic reproduction number $\mathcal{R}_0$

Under some suitable assumptions on the functions b_x and d_x, $x \in \{h, v\}$, one can show that system (4) has a unique positive disease free equilibrium point given by $\mathcal{E}^0 = \left(N_h^0, 0, 0, 0, N_v^0, 0\right)$, where $\left(N_h^0, N_v^0\right)$ is the positive solution of

$$\begin{cases} b_h(N_h^0) - d_h(N_h^0)N_h^0 = 0 \\ b_v(N_v^0) - d_v(N_v^0)N_v^0 = 0. \end{cases} \tag{5}$$

We note that such mathematical assumptions are demographically meaningful and are currently often used in the literature. They are, however, not satisfied for the simplest case of the Malthusian demography, which, therefore, requires a separate analysis, see section 3.3.

By using *the next-generation matrix method* based on the approach and notations used in [16, 38], we find that the control reproduction number, $\mathcal{R}_c$, evaluated at $\mathcal{E}^0$ is given by

$$\mathcal{R}_c = \sqrt{\frac{A_h A_v N_v^0 \left(g_r^0 + f_r \xi_r\right)}{N_h^0 d_v^0 g_i^0 g_r^0}} = \sqrt{\frac{A_h A_v N_v^0 \left[g_r^0 + ((1-c)\omega_h + \sigma)\xi_r\right]}{N_h^0 d_v^0 g_i^0 g_r^0}}, \tag{6}$$

where $b_h^0 = b_h(N_h^0)$, $d_h^0 = d_h(N_h^0)$, $g_i^0 = g_i(N_h^0)$, $g_r^0 = g_r(N_h^0)$, $g_p^0 = g_p(N_h^0)$, $b_v^0 = b_v(N_v^0)$ and $d_v^0 = d_v(N_v^0)$.

Remark 3   *1. The control reproduction number can be rewritten in the form*

$$\mathcal{R}_c^2 = \mathcal{R}_v \left(\mathcal{R}_i + \mathcal{R}_r\right), \tag{7}$$

which can be derived as follows. When an infectious mosquito is introduced into a fully susceptible human population, it will infect humans during its average infectious period, $\dfrac{1}{d_v^0}$, at the rate $\dfrac{A_v}{N_h^0}$. The total number of human infected by this mosquito during its entire infectious period is approximately equal to $\mathcal{R}_v = \dfrac{1}{d_v^0} \times \dfrac{A_v}{N_h^0} \times S_h^0$. On the other hand, if an infectious human is introduced into a population of mosquitoes composed only of susceptible ones, during its average infectious period $\dfrac{1}{g_i^0}$, it will infect mosquitoes at the rate $\dfrac{A_h}{N_h^0}$. After its infectious period, a fraction $\dfrac{(1-c)\omega + \sigma}{g_i^0}$ will recover, and during its recovered period, $\dfrac{1}{g_r^0}$, it will infect mosquitoes at the rate $\dfrac{A_h \zeta_r}{N_h^0}$. So the total number of mosquitoes infected by an infectious human will be $\mathcal{R}_i + \mathcal{R}_r$ with

$$\mathcal{R}_i = \frac{1}{g_i^0} \times \frac{A_h}{N_h^0} \times S_v^0 \text{ and } \mathcal{R}_r = \frac{(1-c)\omega + \sigma}{g_i^0} \times \frac{1}{g_r^0} \times \frac{A_h \zeta_r}{N_h^0} \times S_v^0$$

and (7) follows upon noticing that at DFE we have $S_h^0 = N_h^0$ and $S_v^0 = N_v^0$.

2. *The description given in the previous point does not depend on the nature of the function $b_h(N_h)$, but in the particular case of Malthusian growth we can't use this value to determine the local stability of DFE.*

3. *One can see that $\mathcal{R}_c$ is a decreasing function of c, the probability that the TBDs confer 100% reduction in transmission. So, one needs to increase this parameter to control the evolution of the disease.*

4. *$\mathcal{R}_c$ can be written as $\mathcal{R}_c^2 = \mathcal{R}_0^2 \left(1 - \varphi(c)\right)$, where $\mathcal{R}_0 = \sqrt{\dfrac{A_h A_v N_v^0 \left[g_r^0 + (\omega_h + \sigma)\xi_r\right]}{N_h^0 g_v^0 g_i^0 g_r^0}}$ is the basic reproduction number, obtained when $c = 0$ (i.e., with no treatment with TBDs), and $\varphi(c) = \dfrac{c\omega_h \xi_r}{g_r^0 + (\omega_h + \sigma)\xi_r}$ represents the TBD-induced reduction in $\mathcal{R}_0$.*

3.3 The case of the Malthusian growth of the human population

The case when the first equation in (3) describes the Malthusian growth, that is,

$$N'_h = \pi_h N_h - \mu_{1h} N_h - \delta_h I_h := r_h N_h - \delta_h I_h, \tag{8}$$

though arguably the simplest, does not fit into the general theory and thus requires a special treatment. In fact, the disease free population does not have an equilibrium if $r_h = \pi_h - \mu_{1h} > 0$, it has a continuum of equilibria ($N_h^0 = N_0$ for any initial condition N_0 of N) if $r_h = 0$ and it decays to zero if $r_h < 0$.

In this subsection, and in all subsequent cases, we assume that the disease free mosquito population has a single positive globally stable equilibrium.

First we note that if $r_h < 0$, then $N_h(t) \to 0$ as $t \to \infty$, thus from the nonnegativity of solutions, $I_h(t), S_h(t), R_h(t), P_h(t) \to 0$ as $t \to \infty$ irrespective of δ_h. Thus the whole human population is wiped out and we have globally attractive disease-free (but also human-free) equilibrium $(0, 0, 0, 0, N_v^0, 0)$.

Consider now the case $r_h \geq 0$. Consider the first two equations of (4)

$$\begin{cases} N'_h &= r_h N_h - \delta_h I_h, \\ I'_h &= a\beta_{vh} \frac{I_v}{N_h}(N_h - I_h - R_h - P_h) - (\omega_h + \sigma + \mu_{1h} + \delta_h) I_h. \end{cases} \tag{9}$$

We can make the following observations.

Lemma 4 *The number of infectives I_h, and hence the numbers of recovered R_h and protected P_h, remain bounded irrespective of $r_h \geq 0$ and the bound is independent of $N_h(0)$.*

Proof. Using the notation introduced at the beginning of Section 3.1, we see that the second equation in (9) yields

$$I'_h \leq A_h I_{v,\max} - g_i I_h,$$

where the assumption on the vector's demography implies that $\max_{t \geq 0} I_v(t) := I_{v,\max} < \infty$. Hence

$$I_h(t) \leq e^{-g_i t} I_h(0) + \frac{A_h I_{v,\max}}{g_i}(1 - e^{-g_i t}) \leq \max\left\{ I_h(0), \frac{A_h I_{v,\max}}{g_i} \right\}. \tag{10}$$

Further, $I_{v,\max} \leq N_{v,\max} := \max_{t \geq 0} N_v(t)$ and, by the second equation of (3), $N_{v,\max}$ is independent of $N_h(0)$. Thus

$$\max_{t \geq 0} I_h(t) =: I_{h,\max}$$

for a constant $I_{h,\max}$ independent of r_h and $N_h(0)$ and the statement for I_h is proved.

The statement for R_h and P_h follows directly from (4). ∎

Corollary 5 *There is no globally stable equilibrium for (4) if $r_h > 0$.*

Proof. Since $I_h(t) \leq I_{h,\max}, t \geq 0$, we have

$$N'_h = r_h N_h - \delta_h I_h \geq r_h N_h - \delta_h I_{h,\max}$$

and, as above,

$$N_h(t) \geq e^{r_h t} N_h(0) + \frac{\delta_h I_{h,\max}}{r_h}(1 - e^{r_h t}) = e^{r_h t}\left(N_h(0) - \frac{\delta_h I_{h,\max}}{r_h} \right) + \frac{\delta_h I_{h,\max}}{r_h}.$$

Hence, the population will tend to infinity if we take sufficiently large initial population $N_h(0)$. ∎

Proposition 6 *If $\delta_h < r_h$, then $I_v(t) \to 0$ as $t \to \infty$.*

Proof. We have

$$N_h' \geq (r_h - \delta_h)N_h,$$

so, denoting $\eta = r_h - \delta_h$,

$$N_h \geq N_h(0)e^{\eta t}.$$

Consider the last equation in (4), written as

$$I_v' = A_v \frac{(I_h + \zeta_r R_h)}{N_h} N_v - \left(A_v \frac{(I_h + \zeta_r R_h)}{N_h} + \mu_v \right) I_v.$$

Using Lemma 4, non-negativity of solutions and the boundedness of N_v, we have

$$I_v(t) \leq e^{-\mu_v t} I_v(0) + \frac{K}{\mu_v - \eta} \left(e^{-\eta t} - e^{-\mu_v t} \right)$$

for some constant K, with an obvious modification if $\eta = \mu_v$. ∎

Corollary 7 *Under assumptions of Proposition 6, $I_h(t) \to 0$ as $t \to \infty$.*

Proof. As above, we transform the second equation of (9) as follows

$$I_h' \leq A_h I_v - g_i I_h$$

and obtain

$$I_h(t) \leq e^{-g_i t} I_h(0) + \frac{e^{-g_i t}}{A_h} \int_0^t e^{g_i s} I_v(s)ds$$

and we obtain the thesis either by direct integration or by applying L'Hôspital rule. ∎

Proposition 8 *If $r_h = 0$, then $I_h(t) \to 0$ as $t \to \infty$ and, moreover,*

$$\int_0^\infty I_h(s)ds \leq \frac{N_h(0)}{\delta_h}.$$

Proof. If we take $N = S_h + I_h + R_h + P_h + S_v + I_v$ as a Lyapunov function for (1), we obtain

$$N' = -\delta_h I_h.$$

Since, by Lemma 4, the trajectories are bounded, LaSalle's principle shows that all positive trajectories converge to the largest invariant set contained in $\{(S_h, I_h, R_h, P_h, S_v, I_v) \in \mathbb{R}_+^6 : I_h = 0\}$ and hence $I_h(t) \to 0$ as $t \to \infty$. ∎

Summarizing, if $r_h = 0$, the disease will be eliminated but we do not have criterion which would ensure the survival of the whole population, that is, that $N_h \to N_\infty > 0$ and $t \to \infty$. On the other hand, if $r_h = \pi_h - \mu_{1h} > \delta_h$, then there is no asymptotically stable equilibrium for the whole system (4) as the population is growing unboundedly, however, the numbers of infective hosts and vectors (and hence of recovered and protected humans) tend to zero, and thus we can talk about elimination of the disease. Finally, if $0 < r_h < \delta_h$

3.4 Endemic equilibrium points

The endemic equilibrium point is any point $EEP = (S_h^*, I_h^*, R_h^*, P_h^*, S_v^*, I_v^*)$ solving the system

$$
\begin{cases}
b_h^* + \gamma_h R_h^* + \vartheta_h P_h^* - \left(A_h \dfrac{I_v^*}{N_h^*} + d_h^* \right) S_h^* = 0, \\[2mm]
A_h \dfrac{I_v^*}{N_h^*} S_h^* - g_i^* I_h^* = 0, \\[2mm]
f_r I_h^* - g_r^* R_h^* = 0, \\[2mm]
c\omega_h I_h^* - g_p^* P_h^* = 0, \\[2mm]
b_v^0 - \left(A_v \dfrac{(I_h^* + \zeta_r R_h^*)}{N_h^*} + d_v^0 \right) S_v^* = 0, \\[2mm]
A_v \dfrac{(I_h^* + \zeta_r R_h^*)}{N_h^*} S_v^* - d_v^0 I_v^* = 0.
\end{cases}
$$

where $b_h^* = b_h(N_h^*), d_h^* = d_h(N_h^*), g_i^* = g_i(N_h^*), g_r^* = g_r(N_h^*)$ and $g_p^* = g_p(N_h^*)$. We obtain

$$
R_h^* = \frac{f_r}{g_r^*} I_h^*, \qquad P_h^* = \frac{c\omega_h}{g_p^*} I_h^*, \qquad I_v^* = \frac{A_v \left(1 + \frac{\zeta_r f_r}{g_r^*} \right) I_h^* N_v^0}{A_v \left(1 + \frac{\zeta_r f_r}{g_r^*} \right) I_h^* + d_v^0 N_h^*},
$$

where $S_v^* = N_v^0 - I_v^*$. Using the equation $A_h \dfrac{S_h^*}{N_h^*} I_v^* - g_i^* I_h^* = 0 \Leftrightarrow A_h(N_h^* - P_h^* - R_h^* - I_h^*)I_v^* - g_i^* I_h^* N_h^* = 0$, and after some calculations, we obtain

$$
I_h^* = \frac{g_i^* d_v^0 N_h^{*2} \left(\mathcal{R}_c^{*2} - 1 \right)}{A_v \left(1 + \frac{\zeta_r f_r}{g_r^*} \right) \left(A_h \left(1 + \frac{f_r}{g_r^*} + \frac{c\omega_h}{g_p^*} \right) N_v^0 + g_i^* N_h^* \right)} \tag{11}
$$

with

$$
\mathcal{R}_c^* = \sqrt{\frac{A_h A_v \left(1 + \frac{f_r \zeta_r}{g_r^*} \right) N_v^0}{g_i^* d_v^0 N_h^*}}.
$$

We note that when $\delta_h = 0$, the first equation of (3) becomes $\dfrac{dN_h}{dt} = b_h(N_h) - d_h(N_h)N_h$. In this case, we have $N_h^* = N_h^0$. Therefore, $b_h^* = b_h^0, d_h^* = d_h^0, g_i^* = g_i^0, g_r^* = g_r^0$ and $g_p^* = g_p^0$, which implies that $\mathcal{R}_c^{*2} = \dfrac{A_h N_v^0 A_v \left(1 + \frac{\zeta_r f_r}{g_r^0} \right)}{g_i^0 d_v^0 N_h^0} = \mathcal{R}_c^2$. Hence, (11) can be written as

$$
I_h^* = \frac{g_i^0 d_v^0 N_h^{02} \left(\mathcal{R}_c^2 - 1 \right)}{A_v \left(1 + \frac{\zeta_r f_r}{g_r^0} \right) \left(A_h \left(1 + \frac{f_r}{g_r^0} + \frac{c\omega_h}{g_p^0} \right) N_v^0 + g_i^0 N_h^* \right)}.
$$

This leads to the following result:

Proposition 9 *If $\delta_h = 0$, then system (1) exhibits a forward bifurcation; that is, system (1) has:*

1. *no endemic equilibrium points if $\mathcal{R}_c^2 \in [0,1]$,*

2. *a unique endemic equilibrium point if $\mathcal{R}_c^2 \in (1, +\infty)$.*

Next, we assume that $\delta_h > 0$ and find N_h^* for two particular cases:

3.4.1 Case $d_h(N_h) = \mu_{1h}$

Using the expression of d_h^*, we obtain $g_r^* = g_r^0 = \gamma_h + \mu_{1h}, g_p^* = g_p^0 = \vartheta_h + \mu_{1h}$ and $g_i^* = g_i^0 = \omega_h + \sigma + \delta_h + \mu_{1h}$, which implies that $\mathcal{R}_c^{*2} = \dfrac{A_h N_v^0 A_v \left(1 + \frac{\xi_r f_r}{g_r^0}\right)}{g_i^0 d_v^0 N_h^*}$. Therefore, (11) can be written as

$$I_h^* = \frac{N_h^* \left(A_h N_v^0 \rho - g_i^0 d_v^0 N_h^*\right)}{(\theta N_v^0 + g_i^0 N_h^*)\rho}, \tag{12}$$

where $\rho = A_v \left(1 + \frac{\xi_r f_r}{g_r^0}\right)$ and $\theta = A_h N_v^0 \left(1 + \frac{f_r}{g_r^0} + \frac{c\omega_h}{g_p^0}\right)$.

Remark 10 *If we return to Section 3.3, that is, with $b_h(N_h) = r_h N_h$, then (12) and the stationary case of (8) lead to the following equation for a possible stationary population size*

$$r_h N_h^* - \delta_h \frac{N_h^* \left(A_h \rho N_v^0 - g_i^0 d_v^0 N_h^*\right)}{\rho \left(\theta N_v^0 + g_i^0 N_h^*\right)} = 0, \tag{13}$$

which, if $N_h^* > 0$, gives

$$N_h^* = \frac{\rho N_v^0 (A_h \delta_h - r_h \theta)}{g_i (A_h G_r^* r_h + \delta_h d_v^0)}.$$

We see that $N_h^* > 0$ provided $\delta_h > r_h \left(1 + \frac{f_r}{g_r^*} + \frac{c\omega_h}{g_p^*}\right)$ so, in particular, δ_h must be bigger than r_h, which is consistent with Corollary 6.

Hence, in particular, in the case of a Malthusian population, large disease-induced rates $\delta_h > r_h$ can stabilize a population what would be exponentially growing in the absence of a disease. However, according to Corollary 5, this stabilization will never be global.

3.4.2 Case: $b_h = \lambda_h$ and $d_h(N_h) = \mu_{1h}$

We first note that, in this case, the first equation of system (5) has a unique positive solution $N_h^0 = \frac{\lambda_h}{\mu_{1h}}$. Using $\mathcal{R}_c^2 = \dfrac{A_h N_v^0 \rho}{N_h^0 d_v^0 g_i^0}$, we can write (12) as

$$I_h^* = \frac{d_v^0 g_i^0 N_h^0 N_h^* \left(\mathcal{R}_c^2 - \frac{N_h^*}{N_h^0}\right)}{(\theta + g_i^0 N_h^*)\rho}.$$

Substituting the expression of I_h^* into the equation $b_h^* - d_h^* N_h^* - \delta_h I_h^* = 0$ and using $\lambda_h = \mu_{1h} N_h^0$, we obtain

$$\mu_{1h} N_h^0 - \mu_{1h} N_h^* - \delta_h \frac{d_v^0 g_i^0 N_h^0 N_h^* \left(\mathcal{R}_c^2 - \frac{N_h^*}{N_h^0}\right)}{(\theta + g_i^0 N_h^*)\rho} = 0. \tag{14}$$

To find the endemic equilibrium points of model system (2) we substitute $\frac{N_h^0}{N_h^*} - 1 = x^*$ into (14) and solve for $x^* > 0$, which is equivalent to finding $N_h^* \in \left(0, N_h^0\right)$ that satisfies (14). In fact, it is easy to see that if $0 < N_h^* < N_h^0$, then $x^* > 0$. Moreover, if $x^* > 0$, then $\frac{N_h^0}{N_h^*} > 1$, which, by $N_h^0 > 0$, implies $0 < N_h^* < N_h^0$. Replacing N_h^* by $\frac{N_h^0}{x^* + 1}$ in equation (18), factorizing and collecting with respect to x^*, we obtain the following equation

$$x^{*2} + b\left(\kappa - \mathcal{R}_c^2\right)x^* + \alpha\left(1 - \mathcal{R}_c^2\right) = 0, \tag{15}$$

where

$$\begin{cases} b = \alpha = \dfrac{\delta_h g_i^0 d_v^0}{\mu_{1h}\theta\rho} > 0, \\[4mm] \kappa = \dfrac{(\theta + N_h^0 g_i^0)\mu_{1h}\rho}{\delta_{,h} g_i^0 d_v^0} > 0. \end{cases} \tag{16}$$

In this case, we can apply Proposition 1 of [34]. We obtain

Proposition 11   *1. If $\kappa \geq 1$, then system (1) exhibits a forward bifurcation; that is, system (1) has:*

(a) no endemic equilibrium points if $\mathcal{R}_c^2 \in [0,1]$,

(b) a unique endemic equilibrium point if $\mathcal{R}_c^2 \in (1,+\infty)$.

2. If $\kappa < 1$, then $0 < Q_c := \dfrac{\kappa b - 2 + 2\sqrt{b(1-\kappa)+1}}{b} < 1$ and system (1) exhibits backward bifurcation; that is, system (1) has:

(a) no endemic equilibrium points if $\mathcal{R}_c^2 \in [0, Q_c)$,

(b) one endemic equilibrium point if $\mathcal{R}_c^2 = Q_c$,

(c) two endemic equilibrium points if $\mathcal{R}_c^2 \in (Q_c, 1)$,

(d) a unique endemic equilibrium point if $\mathcal{R}_c^2 \in [1,+\infty)$.

An illustration of the bifurcation results in Proposition 11 is presented in the following figure:
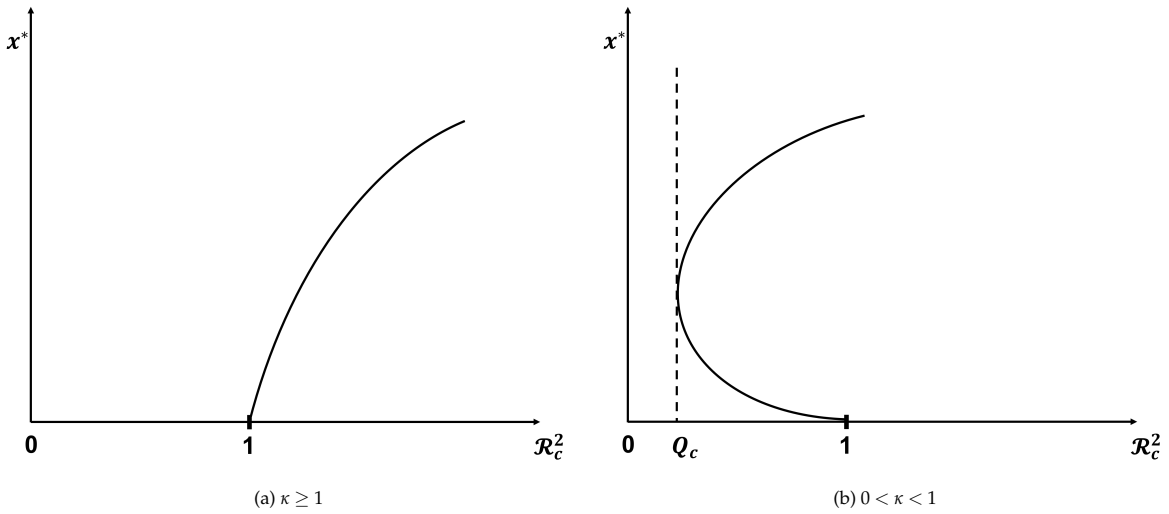

(a) $\kappa \geq 1$ (b) $0 < \kappa < 1$

Figure 3: An illustration of the model's bifurcation behavior.

3.4.3   Case $b_h(N_h) = rN_h\left(1 - \dfrac{N_h}{K}\right)$ and $d_h(N_h) = \mu_{1h}$

We first note that, in this case, the solutions of the first equation of system (5), $rN_h\left(1 - \dfrac{N_h}{K}\right) - \mu_{1h}N_h = 0$, are 0 and $N_h^0 = \dfrac{(r - \mu_{1h})K}{r}$, which is biologically feasible if $r > \mu_{1h}$. One can show that, under this condition, and in the absence of the disease, the human population will converge to N_h^0. Subsequently, in this section, we restrict our analysis to the case where $r > \mu_{1h}$. For notational convenience, we set $\eta = r - \mu_{1h}$.

In this case, N_h^* satisfies

$$rN_h^*\left(1 - \frac{N_h^*}{K}\right) - \mu_{1h}N_h^* - \delta_h \frac{N_h^*\left(A_h N_v^0 \rho - g_i^0 d_v^0 N_h^*\right)}{(\theta + g_i^0 N_h^*)\rho} = 0, \tag{17}$$

Therefore, $N_h^* = 0$, or

$$N_h^{*2} + q_1 N_h^* + q_0 = 0, \tag{18}$$

where

$$
\begin{cases}
q_0 = \dfrac{K\left(\delta_h N_h^0 d_v^0 g_i^0 \mathcal{R}_c^2 - \eta\theta\rho\right)}{r\rho g_i^0} = \dfrac{K\delta_h N_h^0 d_v^0}{r\rho}\left(\mathcal{R}_c^2 - \dfrac{r\theta\rho}{K\delta_h d_v^0 g_i^0}\right), \\[4mm]
q_1 = \dfrac{r\theta\rho - Kg_i^0\left(\eta\rho + \delta_h d_v^0\right)}{r\rho g_i^0} = \dfrac{\theta}{g_i^0} - \dfrac{K\delta_h d_v^0}{r\rho} - N_h^0.
\end{cases}
$$

As in the previous case, we replace N_h^* by $\dfrac{N_h^0}{x^* + 1}$, this leads to the following equation

$$Q_2 x^{*2} + Q_1 x^* + Q_0 = 0, \tag{19}$$

where $Q_0 = \dfrac{r\rho}{K\delta_h N_h^0 d_v^0}\left(N_h^0\left(N_h^0 + q_1\right) + q_0\right) = \dfrac{r\rho}{K\delta_h N_h^0 d_v^0}\left(\dfrac{\theta N_h^0}{g_i^0} + q_0\right), Q_1 = \dfrac{r\rho}{K\delta_h N_h^0 d_v^0}\left(q_1 N_h^0 + 2q_0\right)$ and $Q_2 = \dfrac{r\rho}{K\delta_h N_h^0 d_v^0}q_0$.

Substituting q_0 and q_1 in Q_0 and Q_1, we obtain

$$
\begin{cases}
Q_0 = \mathcal{R}_c^2 - 1 \\
Q_1 = 2\left(\mathcal{R}_c^2 - \kappa_1\right) \\
Q_2 = \mathcal{R}_c^2 - \kappa_2
\end{cases}
$$

where

$$\kappa_1 = \dfrac{r\rho(\theta + g_i^0 N_h^0) + K\delta_h d_v^0 g_i^0}{2K\delta_h d_v^0 g_i^0} > 0 \text{ and } \kappa_2 = \dfrac{r\theta\rho}{K\delta_h d_v^0 g_i^0} > 0.$$

Let

$$\Delta\left(\mathcal{R}_c^2\right) = Q_1^2 - 4Q_0 Q_2 = 4\left(\left(\kappa_2 - 2\kappa_1 + 1\right)\mathcal{R}_c^2 + \left(\kappa_1^2 - \kappa_2\right)\right).$$

One can easily show that $\kappa_1^2 - \kappa_2 > 0$, therefore,

- If $\kappa_2 - 2\kappa_1 + 1 > 0$, then $\Delta\left(\mathcal{R}_c^2\right) > 0$ for all $\mathcal{R}_c$.

- If $\kappa_2 - 2\kappa_1 + 1 < 0$, then $\Delta\left(\mathcal{R}_c^2\right) > 0$ if and only if $\mathcal{R}_c^2 < \kappa_3 := \dfrac{\kappa_2 - \kappa_1^2}{\kappa_2 - 2\kappa_1 + 1}$.

Noting that $\kappa_1 > \kappa_2$ if and only if $\kappa_4 := \dfrac{K\delta_h d_v^0 g_i^0 + r\rho g_i^0 N_h^0}{r\theta\rho} > 1$, we discuss the following two cases.

Case $\kappa_4 > 1$. In this case, $\kappa_1 > \kappa_2$, leading to the following result.

Proposition 12   *1. If $1 < \kappa_2$, then equation (19) has*

    (a) no positive roots if $\mathcal{R}_c^2 < 1$,

    (b) a unique positive root if $1 < \mathcal{R}_c^2 < \kappa_2$,

    (c) two positive roots if $\kappa_2 < \mathcal{R}_c^2 < \kappa_3$,

    (d) no positive roots if $\kappa_3 < \mathcal{R}_c^2$.

  2. If $\kappa_2 < 1 < \kappa_1$, then equation (19) has

    (a) no positive roots if $\mathcal{R}_c^2 < \kappa_2$,

    (b) a unique positive root if $\kappa_2 < \mathcal{R}_c^2 < 1$,

    (c) two positive roots if $1 < \mathcal{R}_c^2 < \kappa_3$,

(d) no positive roots if $\kappa_3 < \mathcal{R}_c^2$.

3. If $\kappa_1 < 1$, then equation (19) has

   (a) no positive roots if $\mathcal{R}_c^2 < \kappa_2$,

   (b) a unique positive root if $\kappa_2 < \mathcal{R}_c^2 < 1$,

   (c) no positive roots if $1 < \mathcal{R}_c^2$.

Proof. We first note that if $\kappa_1 > 1$ and $\kappa_1 > \kappa_2$, then $2\kappa_1 - 1 > \kappa_1$, which, together with $\kappa_2 < \kappa_1$, implies that $\kappa_2 < 2\kappa_1 - 1$. Therefore $\Delta\left(\mathcal{R}_c^2\right) > 0$ if and only if $\mathcal{R}_c^2 < \kappa_3 := \frac{\kappa_2 - \kappa_1^2}{\kappa_2 - 2\kappa_1 + 1}$. Furthermore, $\kappa_3 - \kappa_1 = -\frac{(\kappa_1 - 1)(\kappa_1 - \kappa_2)}{(2\kappa_1 - 1) - \kappa_2} < 0$ and $\kappa_3 - \kappa_2 = \frac{(\kappa_1 - \kappa_2)^2}{(2\kappa_1 - 1) - \kappa_2} > 0$, implying that $\kappa_2 < \kappa_3 < \kappa_1$.

1. If $1 < \kappa_2$, then $\kappa_2 - 2\kappa_1 + 1 = \kappa_2 - \kappa_1 - \kappa_1 + 1 < 0$ (because $\kappa_2 - \kappa_1 < 0$ and $-\kappa_1 + 1 < 0$). This implies that $\Delta\left(\mathcal{R}_c^2\right) > 0$ if and only if $\mathcal{R}_c^2 < \kappa_3 := \frac{\kappa_2 - \kappa_1^2}{\kappa_2 - 2\kappa_1 + 1}$. Furthermore, $\kappa_3 - \kappa_1 = -\frac{(\kappa_1 - 1)(\kappa_1 - \kappa_2)}{(2\kappa_1 - 1) - \kappa_2} < 0$ and $\kappa_3 - \kappa_2 = \frac{(\kappa_1 - \kappa_2)^2}{(2\kappa_1 - 1) - \kappa_2} > 0$, implying that $\kappa_2 < \kappa_3 < \kappa_1$. Thus, we explore the following cases.

   (a) If $\mathcal{R}_c^2 < 1$, then $\mathcal{R}_c^2 < \kappa_1$ and $\mathcal{R}_c^2 < \kappa_2$, implying that $Q_0 > 0, Q_1 > 0$ and $Q_2 > 0$. In this case equation (19) does not have a positive root.

   (b) If $1 < \mathcal{R}_c^2 < \kappa_2$, then $Q_0 > 0$ and $Q_2 < 0$. In this case, equation (19) has a unique positive root.

   (c) If $\kappa_2 < \mathcal{R}_c^2 < \kappa_3$, then $\Delta\left(\mathcal{R}_c\right) > 0$ implying that (19) has two real roots $x_{\pm}^* = \frac{-Q_1 \pm \sqrt{\Delta}}{2Q_0}$, which are positive because, in this case, $Q_0 > 0$, $Q_1 < 0$ and $Q_2 > 0$.

   (d) If $\kappa_3 < \mathcal{R}_c^2$, then, (19) has no positive roots. In fact,

      i. If $\kappa_3 < \mathcal{R}_c^2 < \kappa_1$, then $\Delta\left(\mathcal{R}_c\right) < 0$ implying that (19) has no real roots.

      ii. If $\kappa_1 < \mathcal{R}_c^2$, then $Q_0 > 0$, $Q_1 > 0$ and $Q_2 > 0$. In this case equation (19) does not have a positive root.

2. If $\kappa_2 < 1 < \kappa_1$, then,

   (a) If $\mathcal{R}_c^2 < \kappa_2$, then $Q_0 < 0, Q_1 < 0$ and $Q_2 < 0$. In this case, equation (19) has no positive roots.

   (b) If $\kappa_2 < \mathcal{R}_c^2 < 1$, then $Q_0 < 0$ and $Q_2 > 0$. In this case, equation (19) has a unique positive root.

   (c) If $1 < \mathcal{R}_c^2 < \kappa_3$, then, just like case 1.c., we have $\Delta\left(\mathcal{R}_c\right) > 0$ implying that equation (19) has two roots, which are positive because $Q_0 > 0$, $Q_1 < 0$ and $Q_2 > 0$.

   (d) If $\kappa_3 < \mathcal{R}_c^2$, then just like case 1.d., equation (19) has no positive roots. In fact,

      i. If $\kappa_3 < \mathcal{R}_c^2 < \kappa_1$, then $\Delta\left(\mathcal{R}_c\right) < 0$ implying that (19) has no real roots.

      ii. If $\kappa_1 < \mathcal{R}_c^2$, then $Q_0 > 0$, $Q_1 > 0$ and $Q_2 > 0$. In this case equation (19) does not have a positive root.

3. If $\kappa_1 < 1$, then

   (a) If $\mathcal{R}_c^2 < \kappa_2$, then $Q_0 < 0, Q_1 < 0$ and $Q_2 < 0$. In this case, equation (19) has no positive roots.

   (b) If $\kappa_2 < \mathcal{R}_c^2 < 1$, then $Q_0 < 0$ and $Q_2 > 0$. In this case, equation (19) has a unique positive root.

   (c) If $1 < \mathcal{R}_c^2$, then $Q_0 > 0$, $Q_1 > 0$ and $Q_2 > 0$. In this case, equation (19) has no positive roots.

This completes the proof. ∎

Case $\kappa_4 < 1$. In this case, $\kappa_1 < \kappa_2$ leading to the following result.

Proposition 13   *1. If $1 < \kappa_1$, then equation (19) has*

     (a) no positive roots if $\mathcal{R}_c^2 < 1$,

     (b) a unique positive root if $1 < \mathcal{R}_c^2 < \kappa_2$,

     (c) no positive roots if $\kappa_2 < \mathcal{R}_c^2$.

  2. If $\kappa_1 < 1 < \kappa_2$, then equation (19) has

     (a) no positive roots if $\mathcal{R}_c^2 < \kappa_3$,

     (b) two positive roots if $\kappa_3 < \mathcal{R}_c^2 < 1$.

     (c) a unique positive root if $1 < \mathcal{R}_c^2 < \kappa_2$,

     (d) no positive roots if $\kappa_2 < \mathcal{R}_c^2$.

  3. If $\kappa_2 < 1$, then equation (19) has

     (a) no positive roots if $\mathcal{R}_c^2 < \kappa_2$,

     (b) a unique positive roots if $\kappa_2 < \mathcal{R}_c^2 < 1$,

     (c) no positive roots if $1 < \mathcal{R}_c^2$.

Proof.

1. If $1 < \kappa_1$, then

   (a) If $\mathcal{R}_c^2 < 1$, then $\mathcal{R}_c^2 < \kappa_1$ and $\mathcal{R}_c^2 < \kappa_2$, implying that $Q_0 < 0, Q_1 < 0$ and $Q_2 < 0$. In this case equation (19) does not have a positive root.

   (b) If $1 < \mathcal{R}_c^2 < \kappa_2$, then $\mathcal{R}_c^2 < \kappa_2$, implying that $Q_0 > 0$ and $Q_2 < 0$. In this case, equation (19) has a unique positive root.

   (c) If $\kappa_2 < \mathcal{R}_c^2$, then $Q_0 > 0, Q_1 > 0$ and $Q_2 > 0$. In this case, equation (19) does not have a positive root.

2. If $\kappa_1 < 1 < \kappa_2$, then

   (a) If $\mathcal{R}_c^2 < \kappa_1$, then $Q_0 < 0, Q_1 < 0$ and $Q_2 < 0$. In this case, equation (19) does not have a positive root.

   (b) If $\kappa_1 < \mathcal{R}_c^2 < 1$, then $Q_0 < 0, Q_1 > 0$ and $Q_2 < 0$. Here, we have $(\kappa_2 - (2\kappa_1 - 1)) = (\kappa_2 - \kappa_1) + (1 - \kappa_1) > 0$, implying that $\Delta(\mathcal{R}_c) > 0$ if and only if $\mathcal{R}_c^2 > \kappa_3$. Moreover, since

$$\kappa_3 - 1 = -\frac{(\kappa_1 - 1)^2}{(\kappa_2 - (2\kappa_1 - 1))} < 0$$
$$\kappa_3 - \kappa_1 = \frac{(\kappa_1 - 1)(\kappa_1 - \kappa_2)}{(\kappa_2 - (2\kappa_1 - 1))} > 0$$

   then $\kappa_1 < \kappa_3 < 1$. Thus

       i. If $\kappa_1 < \mathcal{R}_c^2 < \kappa_3$, then $\Delta(\mathcal{R}_c) < 0$, implying that (19) has no positive roots.

       ii. If $\kappa_3 < \mathcal{R}_c^2 < 1$, then $\Delta(\mathcal{R}_c) > 0$, implying that (19) has two real roots, $x_{\pm}^* = \frac{-Q_1 \pm \sqrt{\Delta}}{2Q_0}$, which are positive because $Q_0 Q_2 > 0$ and $-Q_1 Q_2 > 0$.

   (c) If $1 < \mathcal{R}_c^2 < \kappa_2$, then $Q_0 > 0, Q_1 > 0$ and $Q_2 < 0$, and equation (19) has a unique positive root.

(d) If $\kappa_2 < \mathcal{R}_c^2$, then $Q_0 > 0, Q_1 > 0$ and $Q_2 > 0$. Here, equation (19) does not have a positive root.

3. If $\kappa_2 < 1$, then

   (a) If $\mathcal{R}_c^2 < \kappa_1$, then $Q_0 < 0, Q_1 < 0$ and $Q_2 < 0$ and equation (19) does not have a positive root.

   (b) If $\kappa_1 < \mathcal{R}_c^2 < \kappa_2$, then $Q_0 < 0, Q_1 > 0$ and $Q_2 < 0$. Given that $\frac{Q_0}{Q_2} > 0$ and $\frac{-Q_1}{Q_2} < 0$, then if equation (19) had two real roots then their product is positive and their sum is negative implying that they are negative. Therefore, in this case equation (19) does not have any positive root.

   (c) If $\kappa_2 < \mathcal{R}_c^2 < 1$, then $Q_0 < 0, Q_1 > 0$ and $Q_2 > 0$, and equation (19) has a unique positive root.

   (d) If $1 < \mathcal{R}_c^2$, then $Q_0 > 0, Q_1 > 0$ and $Q_2 > 0$. Here, equation (19) does not have a positive root.

This completes the proof. ∎

Remark 14 *The endemic equilibrium points mentioned in this proposition, are given as solutions to*

$$
\begin{cases}
S_h^* = \dfrac{g_i^* N_h^*}{A_h I_v^*} I_h^*, \\[2ex]
R_h^* = \dfrac{f_r}{g_r^*} I_h^*, \\[2ex]
P_h^* = \dfrac{c\omega_h}{g_p^*} I_h^*, \\[2ex]
I_v^* = \dfrac{A_v \left(1 + \frac{\xi_r f_r}{g_r^*}\right) I_h^* N_v^0}{A_v \left(1 + \frac{\xi_r f_r}{g_r^*}\right) I_h^* + d_v^0 N_h^*}, \\[3ex]
S_v^* = N_v^0 - I_v^*,
\end{cases}
$$

where $N_h^* = \dfrac{N_h^0}{x^* + 1}$ with I_h^* derived from the stationary form of the first equation of (4) as

$$
I_h^* = \frac{b_h(N_h^*) - d_h(N_h^*) N_h^*}{\delta_h} = \frac{r N_h^* \left(N_h^0 - N_h^*\right)}{\delta_h K} = \frac{r N_h^{02} x^*}{\delta_h K (x^* + 1)^2}.
$$

Next, we give an illustration of the bifurcation results in Propositions 12 and 13. For this, we express I_h^* in terms of x^*. Since $I_h^* = \frac{r N_h^{02} x^*}{\delta_h K (x^*+1)^2}$, we have two positive roots,

$$
I_{h_\pm}^* = \frac{r N_h^{02}}{K \delta_h} \frac{\left(\kappa_1 - \mathcal{R}_c^2 \pm \sqrt{\Delta}\right)\left(\mathcal{R}_c^2 - 1\right)}{\left(\kappa_1 - 1 \pm \sqrt{\Delta}\right)^2},
$$

where

$$
\Delta(\mathcal{R}_c) = 4\left((\kappa_2 - 2\kappa_1 + 1)\mathcal{R}_c^2 - \left(\kappa_2 - \kappa_1^2\right)\right).
$$

We note the following:

- Clearly, when $\mathcal{R}_c^2 = 1$, we have $I_{h_\pm}^* = 0$.

- The two real roots $I_{h_\pm}^*$ coincide when $\Delta = 0$, that is when $\mathcal{R}_c^2 = \kappa_3 := \frac{\kappa_2 - \kappa_1^2}{\kappa_2 + 1 - 2\kappa_1}$.

- When $\mathcal{R}_c^2 = \kappa_2$, we have $\left(\kappa_1 - \mathcal{R}_c^2 \pm \sqrt{\Delta}\right) = \kappa_1 - \kappa_2 \pm |\kappa_1 - \kappa_2|$, implying that one of the two real roots $I_{h_\pm}^*$ is equal to 0.

An illustration of the bifurcation results in Proposition 12 is presented in the following figures:
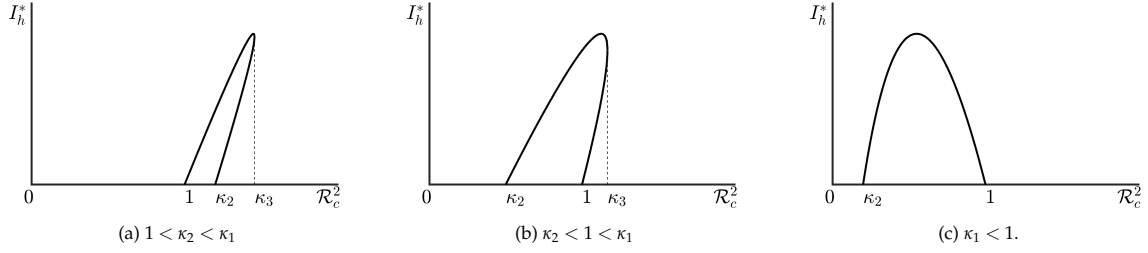

Figure 4: An illustration of the model's bifurcation behavior for $\kappa_2 < \kappa_1$.
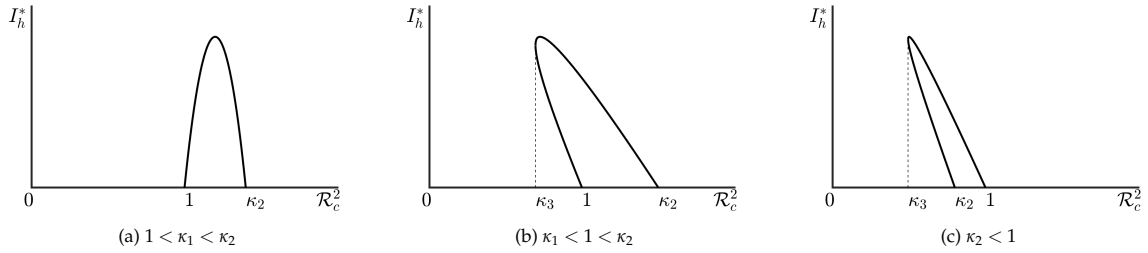

Figure 5: An illustration of the model's bifurcation behavior for $\kappa_1 < \kappa_2$.

Remark 15 *1. As announced in the introduction, we easily see the difference in the model's bifurcation behavior when we change the equation describing the population's demography.*

2. We observe from Propositions 12 and 13 and corresponding Figures 4 and 5 that the model does not always have an endemic equilibrium point even if $\mathscr{R}_c > 1$. This result, not common in SIR models, highlights the complex and counter intuitive ways in which the interplay of the demography and intervention strategies can influence the dynamics of diseases, emphasizing the significance of adopting a comprehensive modeling approach.

We conclude this subsection by deriving the formulae for the endemic equilibrium in the demographic model d) introduced in Section 2. Due to their complexity, however, we only use them in numerical simulations.

3.4.4 Case $b_h(N_h) = \pi_h N_h$ and $d_h(N_h) = \mu_{1h} + \mu_{2h} N_h$

To simplify the expression we set $g_{i_1} = \omega_h + \sigma + \delta_h + \mu_{1h}$, $g_{r_1} = \gamma_h + \mu_{1h}$, $g_{p_1} = \vartheta_h + \mu_{1h}$ and $T_1 = 1 + \dfrac{\zeta_r f_r}{g_r^0}$. In this case with have

$$I_h^* = \frac{\left(\mathscr{R}_c^2 - \frac{(N_h^* \mu_{2h} + g_{i_1})N_h^*}{N_h^0 g_{i_0}}\right) N_h^0 N_h^* d_v^* g_i^0 \left(\frac{f_r \zeta_r}{N_h^* \mu_{2h} + g_{r_1}} + 1\right)}{\left(A_h A_v N_v^* \left(\frac{c\omega_h}{N_h^* \mu_{2h} + g_{p_1}} + \frac{f_r}{N_h^* \mu_{2h} + g_{r_1}} + 1\right)\left(\frac{f_r \zeta_r}{N_h^* \mu_{2h} + g_{r_1}} + 1\right) + \left(N_h^* \mu_{2h} + g_{i_1}\right) A_v N_h^* \left(\frac{f_r}{N_h^* \mu_{2h} + g_{r_1}} + 1\right)\right) T_1}.$$

Hence, by replacing I_h by I_h^* in the equation $b_h(N_h) - d_h(N_h)N_h - \delta_h I_h = 0$, after some algebra we get

$$N_h^* \left(q_5 N_h^{*5} + q_4 N_h^{*4} + q_3 N_h^{*3} + q_2 N_h^{*2} + q_1, N_h^* + q_0\right) = 0 \tag{20}$$

where

$$q_5 = \mu_{2h}^4 \left[d_v^* \delta_h + A_v T_1 \left((\pi_h - \mu_{1h}) - f_r - g_{i_1} - g_{p_1} - 2g_{r_1}\right)\right],$$

17

$$q_4 = -\mu_{2h}^3 A_v T_1 \left[A_h N_v^* \mu_{2h} + g_{r_1} g_{i_1} + g_{r_1} g_{p_1} + f_r \mu_{1h} + (f_r + g_{r_1})(g_{i_1} + g_{r_1} + g_{p_1} - (\pi_h - \mu_{1h})) \right]$$
$$+ \mu_{2h}^3 \delta_h d_v^* (\xi_r f_f g_{i_1} + 2 g_{r_1} + g_{p_1}),$$

$$q_3 = -\mu_{2h} \left[N_h^0 d_v^* \delta_h g_i^0 g_r^0 \mu_{2h} \mathcal{R}_c^2 + A_h A_v N_v^* T_1 \mu_{2h} (c\omega_h + f_r(1 + \xi_r) + 2 g_{p_1} g_{r_1} - (\pi_h - \mu_{1h})) \right.$$
$$+ A_v T_1 \left((g_{i_1} g_{p_1} + g_{i_1} g_{r_1} + g_{r_1} g_{p_1})(f_r + g_{r_1} - (\pi_h - \mu_{1h})) + g_{i_1} g_{p_1} g_{r_1} \right.$$
$$\left. - (\pi_h - \mu_{1h})(f_r + g_{r_1})(g_{i_1} + g_{p_1} + g_{r_1}) \right) - d_v^* \delta_h \left((g_{i_1} + g_{p_1} + g_{r_1})(\xi_r f_r + g_{r_1}) + g_{i_1} g_{p_1} \right) \right],$$

$$q_2 = -\mu_{2h} \left[N_h^0 d_v^* \delta_h \mu_{2h} g_i^0 \mathcal{R}_c^0 (\xi_r f_r + 2 g_{r_1} + g_{p_1}) \right.$$
$$+ A_h A_v N_v^* \mu_{2h} T_1 \left(f_r g_{p_1} + g_{r_1}(c\omega_h + g_{p_1}) + (\xi_r f_r + g_{r_1})(c\omega_h + g_{p_1} + f_r + g_{r_1}) \right.$$
$$\left. - (\pi_h - \mu_{1h})(c\omega_h + g_{p_1} + f_r(\xi_r + 1) + 2 g_{r_1}) \right)$$
$$+ A_v T_1 \left((f_r + g_{r_1})(g_{i_1} g_{p_1} g_{r_1} - (\pi_h - \mu_{1h})(g_{r_1} g_{r_1} + g_{p_1} g_{r_1} + g_{i_1} g_{p_1})) - g_{i_1} g_{p_1} g_{i_1}(\pi_h - \mu_{1h}) \right)$$
$$\left. - d_v^* \delta_h \left((\xi_r f_r + g_{r_1})(g_{r_1} g_{r_1} + g_{p_1} g_{r_1} + g_{i_1} g_{p_1}) + g_{p_1} g_{r_1}^2 \right) \right],$$

$$q_1 = -N_h^0 d_v^* \delta_h \mu_{2h} g_i^0 \mathcal{R}_c^2 \left[g_{p_1} g_{r_1} + (g_{p_1} + g_{r_1})(\xi_r f_r + g_{r_1}) \right]$$
$$+ A_h A_v N_v^* \mu_{2h} T_1 \left[(\xi_r f_r + g_{r_1})((c\omega_h + f_r)(\pi_h - \mu_{1h}) - c\omega_h g_{r_1} - g_{p_1}(f_r + g_{r_1})) \right.$$
$$\left. + (\pi_h - \mu_{1h}) \left((\xi_r f_r + g_{r_1}) g_{p_1} + (g_{r_1} + g_{r_1})(f_r + g_{r_1}) \right) \right] + g_{i_1} g_{p_1} g_{r_1}(f_r + g_{r_1}) \left[A_v T_1 (\pi_h - \mu_{1h}) + d_v^* \delta_h \right],$$

and

$$q_0 = -\delta_h g_{r_1} g_{p_1} g_i^0 N_h^0 d_v^* (\xi_r f_r + g_{r_1}) \left[\mathcal{R}_c^2 - \frac{A_h A_v T_1 N_v^* (\pi_h - \mu_{1h})(c g_{r_1} \omega_h + g_{p_1}(f_r + g_{r_1}))}{\delta_h g_{r_1} g_{p_1} g_i^0 N_h^0 d_v^*} \right].$$

3.5 Global asymptomatic stability of disease free equilibrium (DFE)

In this subsection, we investigate the global asymptomatic stability of disease free equilibrium following the approach in [23] (see also [4, 22]). We proceed by verifying that system (21) satisfies the conditions of Theorem 4.3 in [23]. For this, as in section 3.1, we write the vector $x = (S_h, I_h, R_h, P_h, S_v, I_v)^T$ as (x_s, x_d), with $x_s = (S_h, P_h, S_v)^T$ and $x_d = (I_h, R_h, I_v)^T$, which represent the noninfected and the infected humans and mosquitoes, respectively. With this new notation, model (1) can be written as

$$\begin{cases} x_s' &= A_1(x_s, 0)(x_s - x_s^0) &+ A_{12}(x) x_d \\ x_d' &= &A_2(x) x_d, \end{cases} \tag{21}$$

and we introduce the notation $x_s^0 = \left(N_h^0, 0, N_v^0 \right)$.

Remark 16 *We note the following.*

- *For the case $b_h = \lambda_h$, $b_v = \lambda_v$, $d_h = \mu_{1h}$ and $d_v = \mu_{1v}$, that is, the dynamics of both host and vector populations are given by the simplified logistic model, the disease free equilibrium is given by $\left(N_h^0, 0, N_v^0, 0, 0, 0 \right) = \left(\frac{\lambda_h}{\mu_{1h}}, 0, \frac{\lambda_v}{\mu_{1v}}, 0, 0, 0 \right)$ and*

$$A_1(x_s, 0) = \begin{pmatrix} -\mu_{1h} & \vartheta_h & 0 \\ 0 & -(\vartheta_h + \mu_{1h}) & 0 \\ 0 & 0 & -\mu_{1v} \end{pmatrix}, \quad A_{12}(x) = \begin{pmatrix} 0 & \gamma_h & -A_h \frac{S_h}{N_h} \\ c\omega_h & 0 & 0 \\ -A_v \frac{S_v}{N_h} & -\zeta_r A_v \frac{S_v}{N_h} & 0 \end{pmatrix}.$$

- *For the case $b_h(N_h) = \pi_h N_h$, $b_v(N_v) = \pi_v N_v$, $d_h(N_h) = \mu_{1h} + \mu_{2h} N_h$ and $d_v(N_v) = \mu_{1v} + \mu_{2v} N_v$, we*
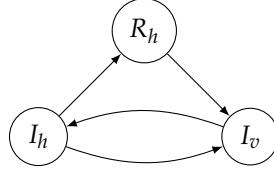
18

Figure 6: Digraph associated to the matrix $A_2(x)$

have the disease free equilibrium given by $\left(N_h^0,0,N_v^0,0,0,0\right) = \left(\frac{\pi_h-\mu_{1h}}{\mu_{2h}},0,\frac{\pi_h-\mu_{1v}}{\mu_{1v}},0,0,0\right)$ *and*

$$A_1(x_s,0) = \begin{pmatrix} -\mu_{2h}N_h & \mu_{1h}+\vartheta_h & 0 \\ 0 & -(\vartheta_h+d(N_h)) & 0 \\ 0 & 0 & -\mu_{2v}N_v \end{pmatrix},$$

$$A_{12}(x) = \begin{pmatrix} \mu_{1h} & \mu_{1h}+\gamma_h & -A_h\dfrac{S_h}{N_h} \\ c\omega_h & 0 & 0 \\ -A_v\dfrac{S_v}{N_h} & -\zeta_r A_v\dfrac{S_v}{N_h} & \mu_{1v} \end{pmatrix}.$$

- *For the case* $b_h(N_h) = rN_h\left(1-\dfrac{N_h}{K}\right)$, $b_v(N_v) = r_vN_v\left(1-\dfrac{N_v}{K_v}\right)$, $d_h(N_h) = \mu_{1h}$ *and* $d_v(N_v) = \mu_{1v}$, *we*

  have the disease free equilibrium given by $\left(N_h^0,0,N_v^0,0,0,0\right) = \left(\dfrac{\eta K}{r},0,K_v\dfrac{r_v-\mu_{1v}}{r_v},0,0,0\right)$ *and*

$$A_1(x_s,0) = \begin{pmatrix} -\dfrac{r}{K}S_h & \dfrac{r}{K}(K-2S_h-P_h)+\vartheta_h & 0 \\ 0 & -(\vartheta_h+\mu_{1h}) & 0 \\ 0 & 0 & -\dfrac{r_v}{K_v}S_v \end{pmatrix},$$

$$A_{12}(x) = \begin{pmatrix} \dfrac{r}{K}(K-2S_h-2P_h-2R_h-I_h) & \dfrac{r}{K}(K-2S_h-2P_h-2R_h)+\gamma_h & -A_h\dfrac{S_h}{N_h} \\ c\omega_h & 0 & 0 \\ -A_v\dfrac{S_v}{N_h} & -\zeta_r A_v\dfrac{S_v}{N_h} & -\dfrac{r_v}{K_v}(K_v-2S_v-I_v) \end{pmatrix}.$$

- *In the general case, we have*

$$A_2(x) = \begin{pmatrix} -g_i(N_h) & 0 & A_h\dfrac{S_h}{N_h} \\ f_r & -g_r(N_h) & 0 \\ A_v\dfrac{S_v}{N_h} & \xi_r A_v\dfrac{S_v}{N_h} & -d_v(N_v) \end{pmatrix}. \tag{22}$$

For the purpose of our global stability analysis, we verify below that assumptions $\mathbf{H}_1$ to $\mathbf{H}_3$ in [23, Theorem 4.3] are verified. In fact, one can prove that

$\mathbf{H}_1$: System(21) is defined on a positively invariant and absorbing set Ω of the non-negative orthant. The system is dissipative on Ω.

$\mathbf{H}_2$: The DFE x^0 of the sub system $x_s' = A_1(x_s,0)(x_s-x_s^0)$ of (21) is globally asymptotically stable on Ω.

$\mathbf{H}_3$: The matrix $A_2(x)$ given by (22) is Metzler. The graph on Figure 6, whose nodes represent the various infected disease states, is strongly connected, which shows that the matrix is irreducible.

We will show next that assumptions $\mathbf{H}_4$ and $\mathbf{H}_5$ are satisfied for the cases of $b_h(N_h)$ and $d_h(N_h)$, discussed in section 5. For the sake of analysis of the global stability, we further assume that

$\tilde{\mathbf{H}}_4$: The equation $b_h(N_h) - (d_h(N_h) + \delta_h)N_h = 0$ has a unique solution $N_h^\#$ in $(0, N_h^0)$.

This, along with $S_h \leq N_h^0$ and $S_v \leq N_v^0$, give the the following upper bound matrix

$$\bar{A}_2 = \begin{pmatrix} -g_i^\# & 0 & A_h \\ f_r & -g_r^\# & 0 \\ A_v \dfrac{N_v^0}{N_h^\#} & \xi_r A_v \dfrac{N_v^0}{N_h^\#} & -d_v^0 \end{pmatrix}.$$

So $A_2(x) \leq \bar{A}_2$, and the equality is possible only when $x = x^0$. Thus, under $\tilde{\mathbf{H}}_4$, assumption $\mathbf{H}_4$ of [23, Theorem 4.3] is satisfied.

We now decompose matrix $\bar{A}_2$ into blocs as

$$\bar{A}_2 = \begin{pmatrix} M & N \\ P & Q \end{pmatrix}$$

where

$$M = -g_i^\#, \quad N = \begin{pmatrix} 0 & A_h \end{pmatrix}, \quad P = \begin{pmatrix} f_r \\ A_v \dfrac{N_v^0}{N_h^\#} \end{pmatrix}, \quad Q = \begin{pmatrix} -g_r^\# & 0 \\ \xi_r A_v \dfrac{N_v^0}{N_h^\#} & -d_v^0 \end{pmatrix},$$

with $g_i^\# = g_i(N_h^\#)$ and $g_r^\# = g_r(N_h^\#)$. Because Q is Metzler stable matrix, we obtain that $\bar{A}_2$ is stable if and only if $M - NQ^{-1}M$ is Metzler stable, that is, $M - NQ^{-1}M$ is negative. Therefore, $\bar{A}_2$ is stable if

$$\frac{A_h A_v N_v^0 \left[g_r^\# + f_r \xi_r \right]}{g_i^\# g_r^\# N_h^\# d_v(N_v^0)} < 1. \tag{23}$$

Since $\mathcal{R}_c^2 = \dfrac{A_h A_v N_v^0 \left[g_r(N_h^0) + ((1-c)\omega_h + \sigma)\xi_r \right]}{N_h^0 d_v(N_v^0) g_i(N_h^0) g_r(N_h^0)}$, $\bar{A}_2$ is stable if and only if

$\tilde{\mathbf{H}}_5$: $\mathcal{R}_c^2 < \mathcal{R}_c^\# := \dfrac{\left(g_r^0 + f_r \xi_r \right) g_i^\# g_r^\# N_h^\#}{\left(g_r^\# + f_r \xi_r \right) g_i^0 g_r^0 N_h^0}.$

We note that $\tilde{\mathbf{H}}_5$ ensures that assumption $\mathbf{H}_5$ of [23, Theorem 4.3] is satisfied, and that due to $\tilde{\mathbf{H}}_4$, we have $R_c^\# < 1$.

The above assumptions ensure that all assumptions of [23, Theorem 4.3] are satisfied. Hence, we have the following result.

Theorem 17 (Global stability of DFE) *The DFE of model* (1) *is globally stable when* $\mathcal{R}_c < \mathcal{R}_c^\#$.

We can also note

Corollary 18 *If* $\delta_h = 0$, *then the coexistence DFE of model* (1) *is globally stable when* $\mathcal{R}_c < 1$.

Proof. If $\delta_h = 0$, then $\kappa > 1$ and $\mathcal{R}_c^\# = 1$ because $N_h^\# = N_h^0$, $g_i(N_h^\#) = g_i(N_h^0)$ and $g_r(N_h^\#) = g_r(N_h^0)$. $\blacksquare$

3.6 Existence of EEPs versus global stability of the DFE

We note that the existence of EEPs is related to the global stability of DFE in the sense that the existence of an EEP for certain values of model's parameters precludes global stability of DFE for these parameters. In this section we show that the results obtained above are consistent, that is, the sets of parameters for which DFE is globally stable and for which there exist EEPs are disjoint.

In Theorem 17, we established that DFE is globally stable when $\mathcal{R}_c < \mathcal{R}_c^{\#}$. However, on Figures 3 – 5, we see that the model admits at least one EEP if $Q^{\#} < \mathcal{R}_c < 1$, where

    i. $Q^{\#} = Q_c$ if $\kappa < 1$,

    ii. $Q^{\#} = \kappa_3$ if $\kappa_1 < \kappa_2$,

    iii. $Q^{\#} = \kappa_2$ if $\kappa_2 < \kappa_1$.

If the inequality $Q^{\#} \leq \mathcal{R}_c^{\#} < 1$ were to hold, then considering $\mathcal{R}_c^2$ within the interval $(Q^{\#}, \mathcal{R}_c^{\#})$ would lead to a contradictory scenario whereby, the model would exhibit both a globally asymptotically disease-free equilibrium point and, at least, one endemic equilibrium point, which is absurd, as noted in the preamble to this section.

Hence, we proceed to demonstrate that $Q^{\#} > \mathcal{R}_c^{\#} < 1$ by analyzing the sign of $Q^{\#} - \mathcal{R}_c^{\#}$. Our calculations are confined to case i., that is:

$$Q^{\#} = Q_c = \frac{\kappa b - 2 + 2\sqrt{b(1-\kappa)+1}}{b},$$

where

$$b = \frac{N_h^0 \delta_h g_i^0 d_v^0}{\mu_{1h}\theta\rho}, \quad \kappa = \frac{\left(\theta + N_h^0 g_i^0\right)\mu_{1h}\rho}{\delta_h g_i^0 d_v^0 N_h^0}.$$

We have the following proposition:

Proposition 19   *1. If $\mathcal{R}_c^{\#} < \frac{2}{\sqrt{b+1}+1}$, then $\mathcal{R}_c^{\#} < Q_c$ for all $\kappa \in (0,1)$*

    2. If $\frac{2}{\sqrt{b+1}+1} < \mathcal{R}_c^{\#}$, then $\kappa^{\#} := \mathcal{R}_c^{\#} - 2\sqrt{\frac{1-\mathcal{R}_c^{\#}}{b}} \in (0,1)$ and we have

        (a) $Q_c > \mathcal{R}_c^{\#}$ for all $\kappa \in (\kappa^{\#}, 1)$,

        (b) $Q_c < \mathcal{R}_c^{\#}$ for all $\kappa \in (0, \kappa^{\#})$.

Proof. Calculating the derivative of Q_c with respect to κ, we obtain $\frac{\partial Q_c}{\partial \kappa} = \frac{b(1-\kappa)}{\sqrt{b(1-\kappa)+1}\left(\sqrt{b(1-\kappa)+1}+1\right)} > 0$ for $\kappa \in (0,1)$. Then the function $\kappa \to Q_c$ increases from $\frac{2}{\sqrt{b+1}+1} < 1$ to 1. Hence,

1. if $\mathcal{R}_c^{\#} < \frac{2}{\sqrt{b+1}+1}$, then $\mathcal{R}_c^{\#} < Q_c$ for all $\kappa \in (0,1)$;

2. if $\frac{2}{\sqrt{b+1}+1} < \mathcal{R}_c^{\#}$, then by letting

$$x = \sqrt{b(1-\kappa)+1} \text{ and } B = \sqrt{b\left(1-\mathcal{R}_c^{\#}\right)},$$

we obtain $\kappa = \frac{1}{b}\left(-x^2 + b + 1\right)$ and

$$Q_c - \mathcal{R}_c^{\#} \quad = \quad \frac{2x - x^2 + B^2 - 1}{b} = \frac{(B - x + 1)(B + x - 1)}{B}.$$

For $\kappa \in (0,1)$, we have $x \in (1, 1+b)$, implying that $B + x - 1 > 0$. Hence $Q_c - \mathcal{R}_c^{\#} = 0$ if and only if $x = B + 1$, that is,

$$\kappa = \kappa^{\#} = \frac{1}{b}\left(-(B+1)^2 + b + 1\right) = \mathcal{R}_c^{\#} - 2\sqrt{\frac{1-\mathcal{R}_c^{\#}}{b}}.$$

We note that since $\mathcal{R}_c^{\#} \to \mathcal{R}_c^{\#} - 2\sqrt{\frac{1-\mathcal{R}_c^{\#}}{b}}$ is increasing and $\frac{2}{\sqrt{b+1}+1} < \mathcal{R}_c^{\#} < 1$, indeed $\kappa^{\#} \in (0,1)$. This leads to the results in 2.(a) and 2.(b). ∎

We can see from this proposition that in cases 1. and 2.(a), we have $Q_c > \mathcal{R}_c^{\#}$, which implies that there is no conflict between the global stability of the DFE and the existence of EEPs. We will skip the calculations in the remaining cases.

4 Numerical simulations

In this section, we run some numerical simulations to monitor the short and long term impact of the disease on four populations of equal size but with different demographics, discussed earlier. Additionally, we investigate how these populations respond to treatment with TBDs. For the sake of our simulations, we set $\omega_h = \phi\omega_{h0}$, where ϕ represents the treatment's coverage and ω_{h0} is the TBD-induced recovery rate. We use the parameter values listed in Table 3. We opt for two specific values of the transmission blocking parameter: $c = 0$ to signify conventional treatments, and $c = 1$ to emulate TBDs. Moreover, we select $\phi = 0.3$ and 0.9 to indicate treatment coverage at low and high levels, respectively. We note that the parameter μ_{1h} is selected to yield an average lifespan of 62 years, whereas λ_h, μ_{2h} and K_h are chosen to ensure that the populations have size equal to $N_h^0 = 10^6$ at equilibrium.

Table 3: Parameters, baseline values, range and references.

Parameters	baseline value or range	reference
Humans		
μ_{1h}	4.4×10^{-5}	Assumed
λ_h	44.19	Assumed
π_h	4.86×10^{-5}	Assumed
μ_{2h}	4.42×10^{-12}	Assumed
r_h	0.001	Assumed
K_h	1.04×10^6	Assumed
β_{hv}	0.24	[11]
a	0.33	[11]
ω_{h0}	3.5×10^{-3}	[8, 11]
c	$(0,1)$	varied
γ_h	0.005	[11]
σ	2×10^{-9}	Assumed
δ_h	0.00047	[32]
ζ_r	0.05	[44]
ϑ_h	0.001	Assumed
Mosquitoes		
π_v	0.13	[4]
λ_v	1×10^4	Assumed
β_{vh}	0.022	[11]
μ_{1v}	0.047	[11]
μ_{2v}	2×10^{-5}	[4]

This leads to

i. $\lambda_h = \mu_{1h}N_h^0$,

ii. $\mu_{2h} = \dfrac{\pi_h - \mu_{1h}}{N_h^0}$,

iii. $K_h = \dfrac{r_h N_h^0}{r_h - \mu_{1h}}$.

We utilize dotted lines to illustrate the model's output in the absence of infection or treatment. The dashed lines are used to depict the output of the model with infection but without treatment, whereas the solid lines includes the treatment. Moreover, different demographic models are associated with colors as follows:

a. blue: $b_h = \lambda_h, d_h = \mu_{1h}$,

b. red: $b_h = r_h N_h(1 - N_h/K_h), d_h = \mu_{1h}$,

c. green: $b_h = \pi_h N_h, d_h = \mu_{1h} + \mu_{2h} N_h$,

d. black: $b_h = \mu_{1h} N_h, d_h = \mu_{1h}$.

4.1 Model without treatment:

The model without treatment is obtained by setting $\phi = 0$. In this case, we have $\mathcal{R}_c^2 = 5.02, \kappa = 630325.08, \kappa_1 = 7.32$ and $\kappa_2 = 10.21$.

Given that $\mathcal{R}_c > 1$,

i. Proposition 11 yields that the blue line in Figure 7(b) will tend to a positive value as t tends to ∞, and

ii. since $1 < \kappa_1 < \kappa_2$ and $1 < \mathcal{R}_c < \kappa_2$, Proposition 13 implies that the red line in Figure 7(b) will tend to a positive value for large values of t.

Furthermore, on Figure 7(b) we observe a substantial difference in the responses to the disease for the populations depicted in blue, red, and black. We also, notice that the blue line displays the highest disease prevalence, followed by the red line, then the black one. The population shown in green exhibits a response to infection similar to that in black; this is partially attributed to the low value of μ_{2h}.

(a)   (b)
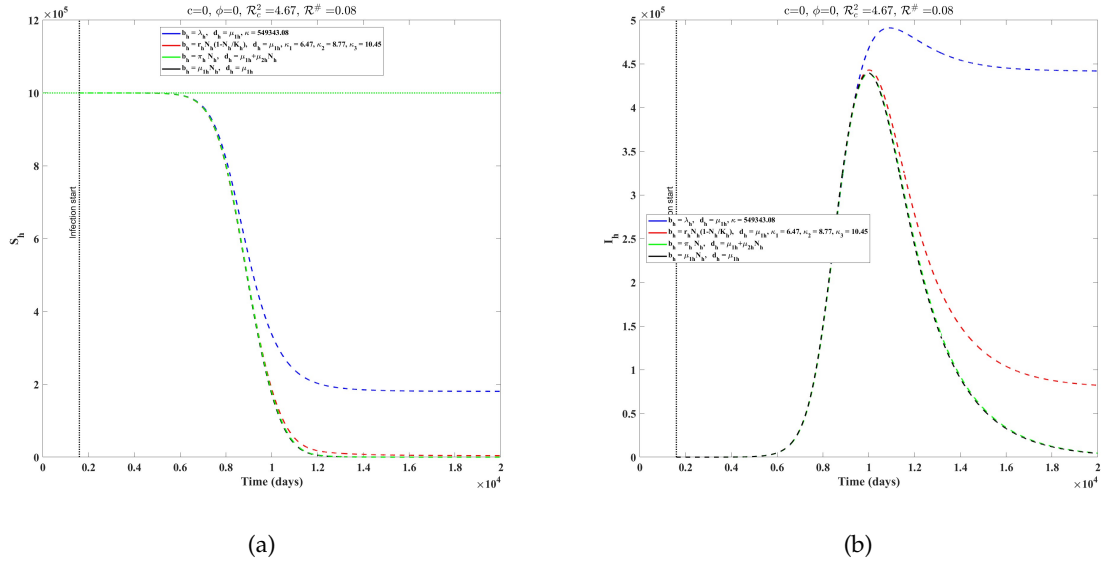
Figure 7: Time evolution of the human population for $\phi = c = 0$. We note the significant difference in the reactions to the disease one the populations represented in blue, red and green. The two population in green and black appear to have similar behaviors.

4.2 Adding Treatment

In this section, we conduct simulations to observe the dynamics of the model under the influence of treatment. We consider two values of the transmission blocking parameter: $c = 0$ for conventional treatments, and $c = 1$ for TBDs. The simulations are performed for two levels of treatment coverage: Low, $\phi = 30\%$ and high, $\phi = 90\%$.

4.2.1 Treatment with conventional drugs, $c = 0$

Low treatment coverage, ϕ=0.3. In this case, $\mathcal{R}_c^2 = 1.68$, $\kappa = 350503.86$, $\kappa_1 = 4.29$ and $\kappa_2 = 4.12$. Given that $\mathcal{R}_c > 1$, we have the following results.

i. From Proposition 11, we obtain that the blue line on Figure 8(b) will tend to a positive value as t tends to ∞. Furthermore, Figure 8(b) illustrates the rapid nature of this convergence, resulting in the disease practically reaching EEP within a reasonable timeframe.

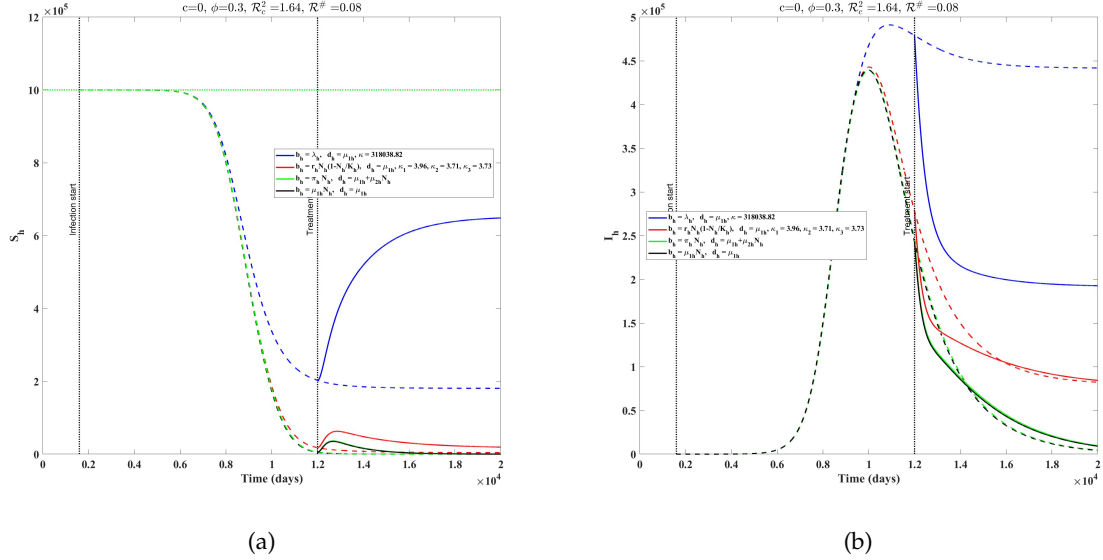ii. Because $1 < \kappa_2 < \kappa_1$ and $1 < \mathcal{R}_c < \kappa_2$ we deduce from Proposition 12 that the red line on Figure 8(b) will tend to a positive value for large values of t. Furthermore, Figure 8(b) illustrates the rapid nature of this convergence, leading to the disease practically reaching EEP within a reasonably short timeframe.

(a)	(b)

Figure 8: Time evolution of the human population for $c = 0$ and $\phi = 0.3$. The graphs indicate a significant difference in the response to treatment.

High treatment coverage, $\phi = 0.9$: In this case, $\mathcal{R}_c^2 = 0.73$, $\kappa = 275085.36$, $\kappa_1 = 3.48$ and $\kappa_2 = 2.42$. Given that $\mathcal{R}_c < 1$, we have the following results.

i. Since $\kappa > 1$, then, from Proposition 11, we obtain that the blue line in Figure 9(b) will tend to zero for large values of t. Furthermore, Figure 9(b) illustrates the rapid nature of this convergence, resulting in disease elimination within a reasonable time.

ii. Because $1 < \kappa_2 < \kappa_1$ and $\mathcal{R}_c < 1$ we deduce from Proposition 12 that the red line in Figure 9(b) will tend to zero when t is large enough. Furthermore, Figure 9(b) illustrates the slow nature of this convergence, leading to the disease persistence even after a reasonably long time.
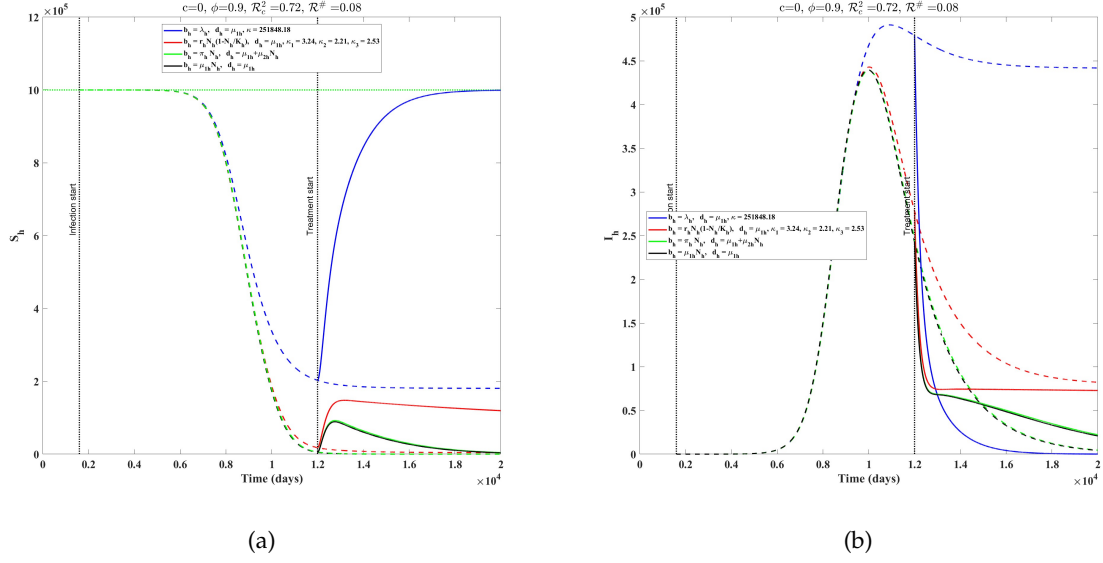
(a)   (b)

Figure 9: Time evolution of the human population for $c = 0$ and $\phi = 0.9$

4.2.2 Treatment with TBDs, $c = 1$

Low treatment coverage, $\phi = 0.3$. In this case, $\mathcal{R}_c^2 = 1.66, \kappa = 470671.58, \kappa_1 = 5.59$ and $\kappa_2 = 6.75$. Given that $\mathcal{R}_c > 1$, then we have the following results.

i. From Proposition 11, we obtain that the blue line on Figure 10(b) will tend to a positive value as t tends to ∞. Furthermore, Figure 10(b) illustrates the rapid nature of this convergence, resulting in the disease reaching EEP within a reasonable time.

ii. Because $1 < \kappa_1 < \kappa_2$ and $1 < \mathcal{R}_c < \kappa_2$ we deduce from Proposition 13 that the red line on Figure 10(b) will tend to a positive value for large values of t. Furthermore, Figure 10(b) illustrates the rapid nature of this convergence, leading to the disease reaching EEP within a reasonably short time.

(a)   (b)
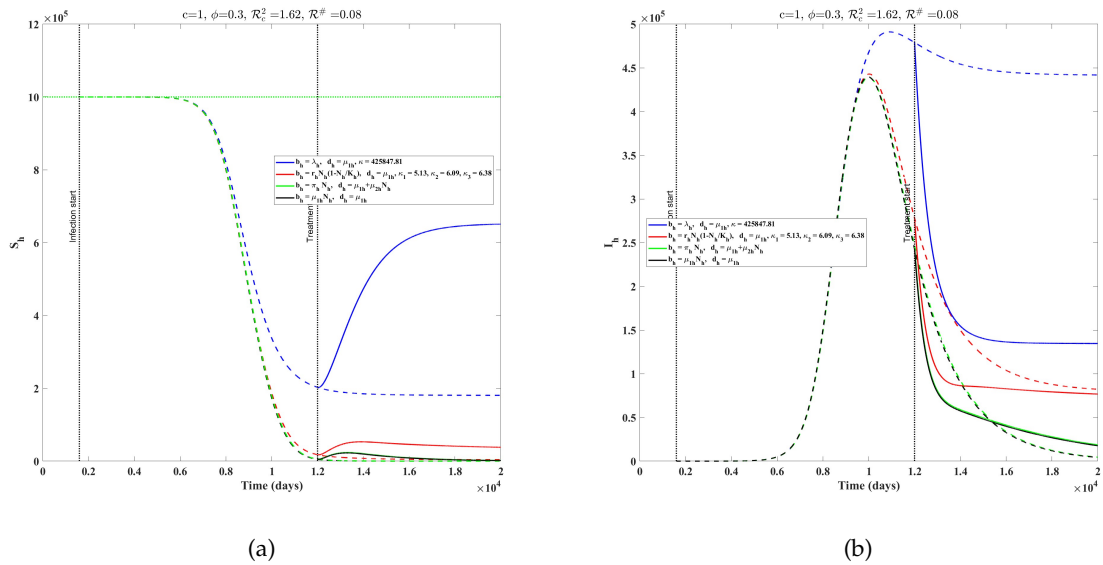
Figure 10: Time evolution of the human population for $c = 1$ and $\phi = 0.3$

25

High treatment coverage, $\phi = 0.9$:   In this case, $\mathcal{R}_c^2 = 0.71, \kappa = 425533.00, \kappa_1 = 5.10$ and $\kappa_2 = 5.78$. Given that $\mathcal{R}_c < 1$, we have the following results.

i. Since $\kappa > 1$, then, from Proposition 11, we obtain that the blue line on Figure 11(b) will be close to zero for large values of t. Furthermore, Figure 11(b) illustrates the rapid nature of this convergence, resulting in disease elimination within a reasonable timeframe.

ii. Because $1 < \kappa_1 < \kappa_2$ and $\mathcal{R}_c < 1$, we deduce from Proposition 13 that the red line on Figure 11(b) will tend to zero when t is large enough. Furthermore, Figure 11(b) illustrates the slow nature of this convergence, leading to the disease persistence even after a reasonably long time.

(a)	(b)
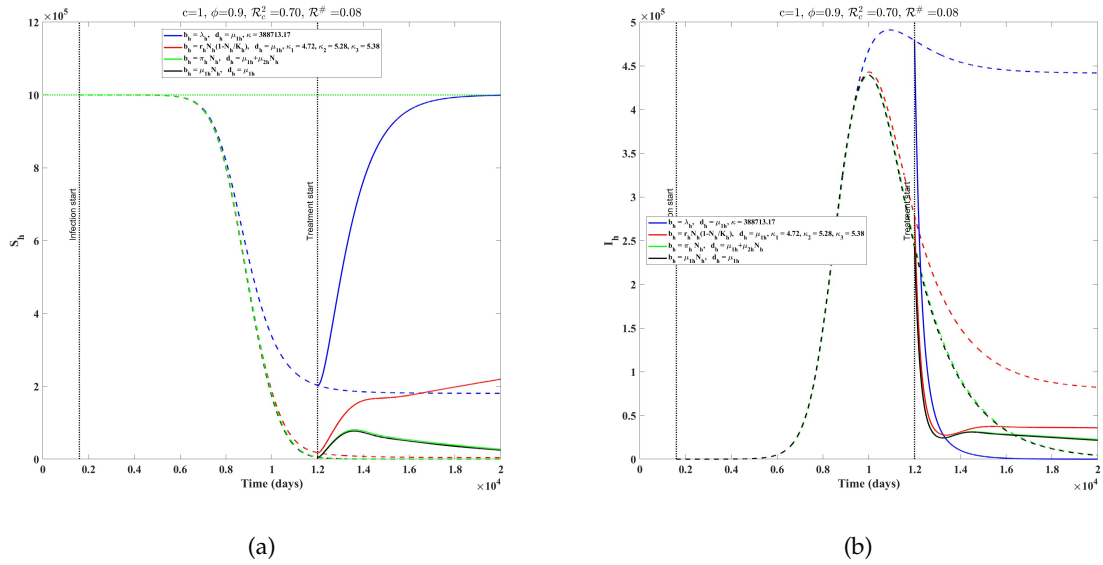
Figure 11: Time evolution of the human population for $c = 1$ and $\phi = 0.9$

Finally, it is worth noting that in each of the Figures 8(b) to 11(b), there is a significant difference between the responses to the treatment for the populations depicted in blue, red and black. Additionally, the blue line exhibits the highest level of disease prevalence, followed by the red line, then the black line. The population shown in green has a response to treatment similar to that in black; this could be explained by the low value of μ_{2h}.

4.2.3   Positive versus Negative

In the previous section, we observed that, under treatment, the blue line presents the highest disease prevalence, followed by the red line, and the black and green lines. Given that, prior to treatment, the disease prevalence was initially higher in the blue than it is for the other lines, it may be relevant to explore the reduction in the burden of the disease caused by the treatment.

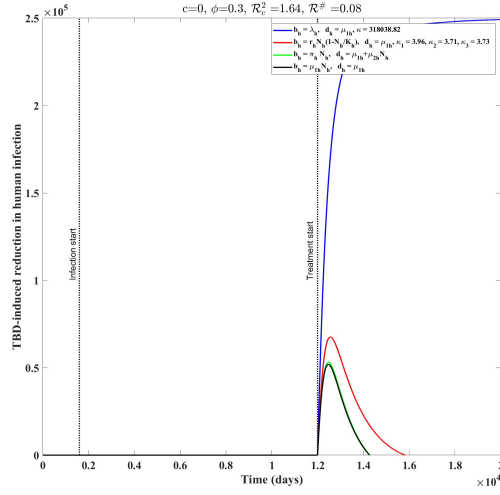For this purpose, we define and plot the "reduction" terms

i. the absolute change in $I_h(t)$, defined as

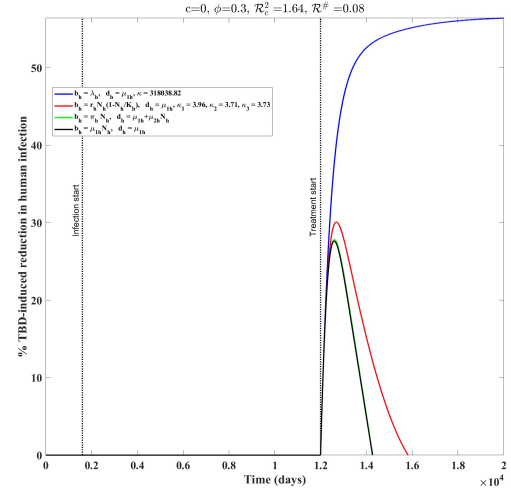$$\Delta I_h(t) := I_h(t) \text{ without treatment } - I_h(t) \text{ with treatment,}$$

and

26

ii. the percentage change in $I_h(t)$, given by

$$\frac{I_h(t) \text{ without treatment } - I_h(t) \text{ with treatment}}{I_h(t) \text{ without treatment}}.$$

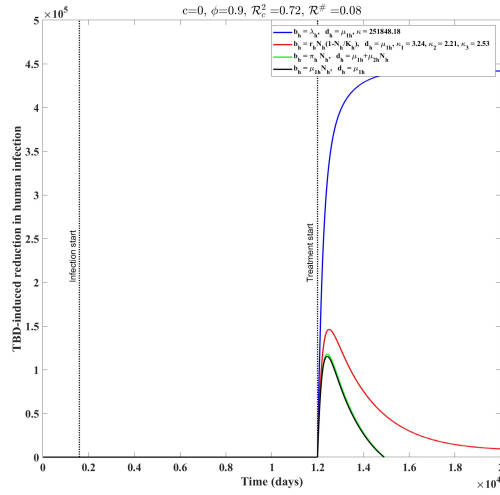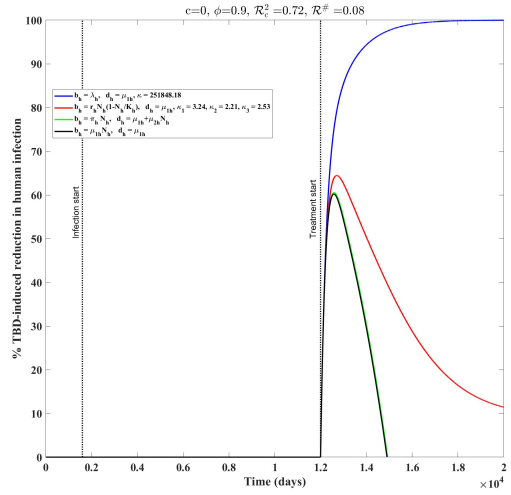(a)   (b)

Figure 12: Time evolution of the reduction in human infection for $c = 0$ and $\phi = 0.3$.

(a)   (b)

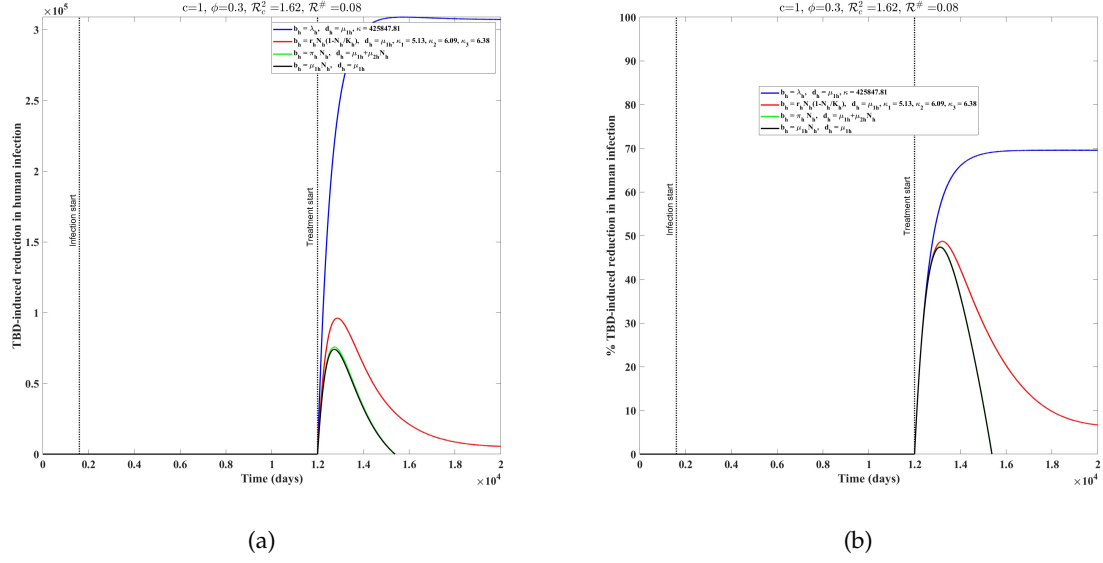Figure 13: Time evolution of the reduction in human infection for $c = 0$ and $\phi = 0.9$

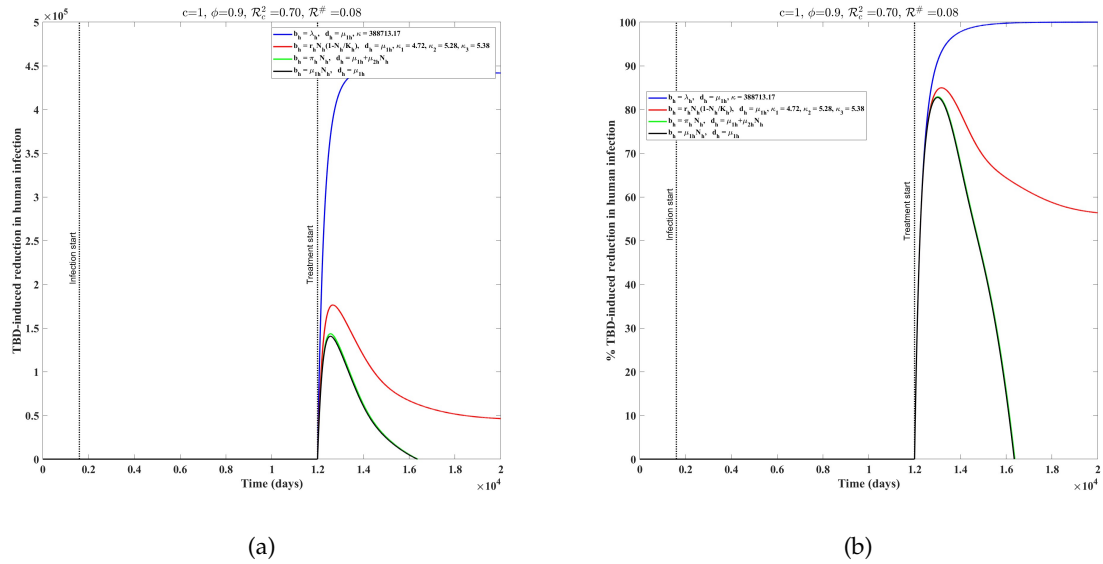Figure 14: Time evolution of the reduction in human infection for $c = 1$ and $\phi = 0.3$

Figure 15: Time evolution of the reduction in human infection for $c = 1$ and $\phi = 0.9$

We note the following.

i. On Figures 12 – 15, the left graphs show that, for all values of c and ϕ, $\Delta I_h(t)$, represented in blue, is positive for all $t \geq 0$, implying that treatment leads to a decrease in the number of cases for this population. The large values of $\Delta I_h(t)$ compared to those of the other lines indicate that population represented in blue undergoes the highest reduction in the number of infected cases. The right graphs indicate that the reduction can exceed 100%. The same goes for the red line on Figures 13 – 15.

In contrast,

ii. On Figures 12 – 15, the left graphs show that, for all values of c and ϕ, $\Delta I_h(t)$, depicted in black and green, becomes negative for a fixed period of time. This means that, for this population, treatment leads to a temporary increase in the number of infected cases. The right graphs indicate

28

an increase in the number of infections exceeding 100%. This also applies to the red line in Figure 12. This apparent paradox can be explained by the fact that the treatment, while temporarily reducing the number of infectives, leads in turn to an increase in the number of susceptibles, which then leads to the increase in the number of infectives.

4.3 Summary

Following a comprehensive mathematical and numerical analysis of the responses of the four populations to both the disease and treatment with TBDs, it is noteworthy to emphasize the following key findings.

i. When the four populations are exposed to malaria, the population represented in blue experiences the highest disease burden. Nonetheless, when treatment with TBDs is used with a high coverage, this population will be the first to eliminate the disease, demonstrating the highest reduction in disease prevalence when compared to the other three populations.

ii. It is observed that, through the application of treatment with TBDs, disease elimination becomes attainable at high coverage levels. Nevertheless, among the four populations, only the one depicted by the blue line successfully achieves disease elimination within a reasonable timeframe.

It is worthwhile to point out that the population in blue, whose behavior differs so significantly from the other three, is described by the simplified logistic, or affine, model. Though very popular in modeling, it is biologically incorrect as it describes populations in which the total birth rate is independent of the size of the population. This feature can explain the outlier behavior observed above as even a dramatic drop in the population size due to the disease does not impact the number of newborn susceptibles, thanks to whom the population rebounds.

5 Conclusion

In this paper, we developed and analyzed a mathematical model for the spread of malaria disease that integrates treatment with Transmission Blocking Drugs (TBDs). The foundation of our model lies in its incorporation of four distinct demographic types, allowing for a more realistic representation of population dynamics and shedding light on their potential significance in disease transmission and control strategies. We calculated the model's control reproduction number and equilibria and performed a global stability analysis of the disease-free equilibrium point. Moreover, we delved into the bifurcation dynamics of the model, unraveling the intricate ways the disease can manifest and spread within different subpopulations. Of paramount importance is our finding that, depending on the population's demography, the model can exhibit a forward bifurcation, a backward one, or even some unconventional types of bifurcations in which the disease can be eliminated either for low or high values of the basic reproduction number ($\mathscr{R}_c$).

This finding challenges commonly accepted beliefs and holds profound implications for disease control strategies. It highlights the potential for disease elimination even in regions with moderate to high transmission potential, given the right intervention strategies and deployment of TBDs.

In addition to analytical exploration, we conducted extensive numerical simulations to validate and expand our findings. Our simulations revealed distinct responses to the disease and TBD treatment among three of the four demographic populations. Remarkably, the demographic group displaying the highest increase in disease prevalence also exhibited the most substantial reduction in disease burden following treatment with TBDs. This counter intuitive observation suggests a complex interplay between demography, disease transmission dynamics and disease control. Furthermore, our simulations

unveiled an intriguing phenomenon whereby the demographic group experiencing the lowest disease burden exhibited a temporary surge in disease prevalence as a direct consequence of TBD intervention. However, these temporary spikes were ultimately followed by a reduction in disease burden.

The above underscores the intricate and sometimes counter intuitive mechanisms through which intervention strategies can impact disease dynamics, underscoring the importance of a comprehensive modeling approach.

In conclusion, our study introduces a comprehensive mathematical model integrating transmission-blocking drugs into the malaria transmission dynamics framework. Our mathematical analysis and numerical simulations uncover novel bifurcation scenarios and intricate demographic responses to disease and intervention strategies. These findings collectively provide a novel understanding of malaria transmission dynamics and offer valuable insights for designing effective and nuanced disease control strategies in diverse demographic settings.

Acknowledgment

Conflict of Interest

All authors declare no potential conflict of interest.

References

[1] Jacob B Aguilar and Juan B Gutierrez. An epidemiological model of malaria accounting for asymptomatic carriers. *Bulletin of Mathematical Biology*, 82(3):1–55, 2020.

[2] Roy M Anderson, B Anderson, and Robert M May. *Infectious diseases of humans: dynamics and control*. Oxford University Press, 1992.

[3] Kayla Ann Andrews, David Wesche, James McCarthy, Jörg J Möhrle, Joel Tarning, Luann Phillips, Steven Kern, and Thaddeus Grasela. Model-informed drug development for malaria therapeutics. *Annual review of pharmacology and toxicology*, 58:567–582, 2018.

[4] Roumen Anguelov, Yves Dumont, Jean Lubuma, and Eunice Mureithi. Stability analysis and dynamics preserving nonstandard finite difference schemes for a malaria model. *Mathematical Population Studies*, 20(2):101–122, 2013.

[5] Joan L Aron and Robert M May. The population dynamics of malaria. In *The population dynamics of infectious diseases: theory and applications*, pages 139–179. Springer, 1982.

[6] Edoardo Beretta, Vincenzo Capasso, and Dario G Garao. A mathematical model for malaria transmission with asymptomatic carriers and two age groups in the human population. *Mathematical biosciences*, 300:87–101, 2018.

[7] Lyn-Marie Birkholtz, Theresa L Coetzer, Dalu Mancama, Didier Leroy, and Pietro Alano. Discovering new transmission-blocking antimalarial compounds: challenges and opportunities. *Trends in parasitology*, 32(9):669–681, 2016.

[8] Michael T Bretscher, Jamie T Griffin, Azra C Ghani, and Lucy C Okell. Modelling the benefits of long-acting or transmission-blocking drugs for reducing plasmodium falciparum transmission by case management or by mass treatment. *Malaria journal*, 16(1):341, 2017.

[9] Iulia Martina Bulai, Stephanie Depickere, and Vitor Hirata Sanches. Influence of asymptomatic people on malaria transmission: A mathematical model for a low-transmission area case. *Journal of Biological Systems*, 28(01):167–182, 2020.

[10] Nakul Chitnis, Jim M Cushing, and JM Hyman. Bifurcation analysis of a mathematical model for malaria transmission. *SIAM Journal on Applied Mathematics*, 67(1):24–45, 2006.

[11] Nakul Chitnis, James M Hyman, and Jim M Cushing. Determining important parameters in the spread of malaria through the sensitivity analysis of a mathematical model. *Bulletin of mathematical biology*, 70(5):1272, 2008.

[12] Derek A T Cummings, Sopon Iamsirithaworn, Justin T Lessler, Aidan McDermott, Rungnapa Prasanthong, Ananda Nisalak, Richard G Jarman, Donald S Burke, and Robert V Gibbons. The impact of the demographic transition on dengue in thailand: insights from a statistical analysis and mathematical modeling. *PLoS Med*, 6(9):e1000139, September 2009.

[13] Ahmed Danbaba. *Mathematical models and analysis for the transmission dynamics of malaria*. PhD thesis, University of Pretoria, 2016.

[14] BA Danquah, F Chirove, and Jacek Banasiak. Effective and ineffective treatment in a malaria model for humans in an endemic region. *Afrika Matematika*, 30(7-8):1181–1204, 2019.

[15] MJ Delves, F Angrisano, and AM Blagborough. Antimalarial transmission-blocking interventions: past, present, and future. *Trends in parasitology*, 34(9):735–746, 2018.

[16] Odo Diekmann, Johan Andre Peter Heesterbeek, and Johan AJ Metz. On the definition and the computation of the basic reproduction ratio r 0 in models for infectious diseases in heterogeneous populations. *Journal of mathematical biology*, 28(4):365–382, 1990.

[17] Klaus Dietz, WH Wernsdorfer, I McGregor, et al. Mathematical models for transmission and control of malaria. *Principles and Practice of Malariology*, pages 1091–1133, 1988.

[18] João AN Filipe, Eleanor M Riley, Christopher J Drakeley, Colin J Sutherland, and Azra C Ghani. Determination of the processes driving the acquisition of immunity to malaria using a mathematical transmission model. *PLoS computational biology*, 3(12):e255, 2007.

[19] Nicholas Geard, Kathryn Glass, James M McCaw, Emma S McBryde, Kevin B Korb, Matt J Keeling, and Jodie McVernon. The effects of demographic change on disease transmission and vaccine impact in a household structured population. *Epidemics*, 13:56–64, September 2015.

[20] Johannes Horn, Oliver Damm, Wolfgang Greiner, Hartmut Hengel, Mirjam E Kretzschmar, Anette Siedler, Bernhard Ultsch, Felix Weidemann, Ole Wichmann, André Karch, and Rafael T Mikolajczyk. Influence of demographic changes on the impact of vaccination against varicella and herpes zoster in germany - a mathematical modelling study. *BMC Med*, 16(1):3, January 2018.

[21] A Meredith John. Endemic disease in host populations with fully specified demography. *Theor Popul Biol*, 37(3):455–471, June 1990.

[22] Jean Claude Kamgang, Vivient Corneille Kamla, Stéphane Yanick Tchoumi, et al. Modeling the dynamics of malaria transmission with bed net protection perspective. *Applied Mathematics*, 5(19):3156, 2014.

[23] Jean Claude Kamgang and Gauthier Sallet. Computation of threshold conditions for epidemiological models and global stability of the disease-free equilibrium (dfe). *Mathematical biosciences*, 213(1):1–12, 2008.

[24] Kim A Lindblade, Laura Steinhardt, Aaron Samuels, S Patrick Kachur, and Laurence Slutsker. The silent threat: asymptomatic parasitemia and malaria transmission. *Expert review of anti-infective therapy*, 11(6):623–639, 2013.

[25] George Macdonald et al. The epidemiology and control of malaria. *The Epidemiology and Control of Malaria.*, 1957.

[26] Valentina Marziano, Piero Poletti, Giorgio Guzzetta, Marco Ajelli, Piero Manfredi, and Stefano Merler. The impact of demographic changes on the epidemiology of herpes zoster: Spain as a case study. *Proc Biol Sci*, 282(1804):20142509, April 2015.

[27] Elamaran Meibalan and Matthias Marti. Biology of malaria transmission. *Cold Spring Harbor perspectives in medicine*, 7(3):a025452, 2017.

[28] Stefano Merler and Marco Ajelli. Deciphering the relative weights of demographic transition and vaccination in the decrease of measles incidence in italy. *Proc Biol Sci*, 281(1777):20132676, January 2014.

[29] Signe Møgelmose, Karel Neels, and Niel Hens. Incorporating human dynamic populations in models of infectious disease transmission: a systematic review. *BMC Infect Dis*, 22(1):862, November 2022.

[30] Gideon A Ngwa and William S Shu. A mathematical model for endemic malaria with variable human and mosquito populations. *Mathematical and Computer Modelling*, 32(7-8):747–763, 2000.

[31] S Olaniyi and OS Obabiyi. Mathematical model for malaria transmission dynamics in human and mosquito populations with nonlinear forces of infection. *International journal of pure and applied Mathematics*, 88(1):125–156, 2013.

[32] World Health Organization et al. World malaria report 2014: summary. Technical report, World Health Organization, 2015.

[33] World Health Organization et al. World malaria report 2019. 2019.

[34] Rachid Ouifki and Jacek Banasiak. Epidemiological models with quadratic equation for endemic equilibria-a bifurcation atlas. *Mathematical Methods in the Applied Sciences*, 43:10413– 10429, 2020.

[35] Ronald Ross. *The prevention of malaria*. Dutton, 1910.

[36] Ruprecht Schmidt-Ott, Markus Schwehm, and Martin Eichner. Influence of social contact patterns and demographic factors on influenza simulation results. *BMC Infect Dis*, 16(1):646, November 2016.

[37] Stéphane Yanick Tchoumi, Herieth Rwezaura, and Jean Michel Tchuenche. A mathematical model with numerical simulations for malaria transmission dynamics with differential susceptibility and partial immunity. *Healthcare Analytics*, 3:100165, 2023.

[38] Pauline Van den Driessche and James Watmough. Reproduction numbers and sub-threshold endemic equilibria for compartmental models of disease transmission. *Mathematical biosciences*, 180(1-2):29–48, 2002.

[39] Ishan Wadi, Anupkumar R Anvikar, Mahendra Nath, C Radhakrishna Pillai, Abhinav Sinha, and Neena Valecha. Critical examination of approaches exploited to assess the effectiveness of transmission-blocking drugs for malaria. *Future medicinal chemistry*, 10(22):2619–2639, 2018.

[40] WHO. World malaria report 2018e. `https://www.who.int/malaria/publications/world-malaria-report-2018/en/`, 2018. Last update: 19 November 2018.

[41] WHO. World malaria report, 2021.

[42] WHO-GHO. Data-malaria. `https://apps.who.int/gho/data/node.main.A1362?lang=en`, 2016. Last updated: 2019-02-12, Acessed: 2020-08-29.

[43] Mark F. Wiser. Malaria. `http://www.tulane.edu/~wiser/protozoology/notes/malaria.html`, 2011.

[44] Woldegebriel Assefa Woldegerima, Rachid Ouifki, and Jacek Banasiak. Mathematical analysis of the impact of transmission-blocking drugs on the population dynamics of malaria. *Applied Mathematics and Computation*, 400:126005, 2021.

[45] Hyun M Yang and Marcelo U Ferreira. Assessing the effects of global warming and local social and economic conditions on the malaria transmission. *Revista de saude publica*, 34(3):214–222, 2000.